American Diabetes Association. diabetes

Hyperglycemia-induced PKCβ2 Activation Induces Diastolic Cardiac Dysfunction in Diabetic Rats by Impairing Caveolin-3 Expression and Akt/eNOS Signaling

Journal:	*Diabetes*
Manuscript ID:	DB12-1391.R1
Manuscript Type:	Original Article
Date Submitted by the Author:	n/a
Complete List of Authors:	Lei, Shaoqing; University of Hong Kong, Department of Anesthesiology Li, Haobo; The University of Hong Kong, Department of Anesthesiology Xu, Jinjin; University of Hong Kong, Department of Anesthesiology Liu, Yanan; University of Hong Kong, Department of Anesthesiology Gao, Xia; University of Hong Kong, Department of Anesthesiology Wang, Junwen; University of Hong Kong, Department of Biochemistry Ng, Kwok; University of Hong Kong, Department of Anesthesiology Lau, Wayne; Thomas Jefferson University, Department of Emergency Medicine Ma, Xin-liang; Thomas Jefferson University, Department of Emergency Medicine Rodrigues, Brian; University of British Columbia, Faculty of Pharmaceutics Irwin, Michael; University of Hong Kong, Department of Anesthesiology Xia, Zhengyuan; University of Hong Kong, Department of Anesthesiology
Key Words:	caveolin-3, Protein Kinase C, Diabetes, Cardiomyopathy

Hyperglycemia-induced PKCβ$_2$ Activation Induces Diastolic Cardiac Dysfunction in Diabetic Rats by Impairing Caveolin-3 Expression and Akt/eNOS Signaling

Shaoqing Lei[1], Haobo Li[1], Jinjin Xu[1], Yanan Liu[1], Xia Gao[1], Junwen Wang [2;3], Kwok F.J. Ng [1;3], Wayne Bond Lau[4], Xin-liang Ma[4], Brian Rodrigues[5], Michael G. Irwin[1;3#]and Zhengyuan Xia[1;3#]

[1]Department of Anesthesiology, [2]Department of Biochemistry, The University of Hong Kong, Hong Kong SAR, China; [3]Shenzhen Institute of Research & Innovation, The University of Hong Kong, Shenzhen, China; [4]Department of Emergency Medicine, Thomas Jefferson University, 1020 Sansom Street, Philadelphia, PA 19107, USA; [5]Faculty of Pharmaceutical Sciences, The University of British Columbia, Vancouver, BC, Canada

Running title: Hyperglycemia induces protein kinase C (PKC) β$_2$ activation

Words count: 4000

Number of figures: 7

#MG Irwin and Z Xia share senior authorship

Address correspondence to:

Dr. Zhengyuan Xia

Department of Anesthesiology, University of Hong Kong, Hong Kong SAR, China

Tel: (852) 28199794; Fax: (852) 2819-9791

E-mail: zyxia@hku.hk

Abstract

Protein kinase C(PKC)β_2 is preferably overexpressed in the diabetic myocardium, which induces cardiomyocyte hypertrophy and contributes to diabetic cardiomyopathy, but the underlying mechanisms ~~is~~ are incompletely understood. Caveolae are critical in signal transduction of PKC isoforms in cardiomyocytes. Caveolin(Cav)-3, the cardiomyocyte-specific caveolar structural protein isoform, is decreased in the diabetic heart. The current study determined whether PKCβ_2 activation affects caveolae and Cav-3 expression. Immunoprecipitation and immunofluorescence analysis revealed that high glucose(HG) increased the association and co-localization of PKCβ_2 and Cav-3 in isolated cardiomyocytes. Disruption of caveolae by methyl-β-cyclodextrin or Cav-3 siRNA transfection prevented HG-induced PKCβ_2 phosphorylation. Inhibition of PKCβ_2 activation by compound CGP53353 or knockdown of PKCβ_2 expression via siRNA attenuated the reductions of Cav-3 expression and Akt/eNOS phosphorylation in cardiomyocytes exposed to HG. LY333531 treatment (for a duration of 4 weeks) prevented excessive PKCβ_2 activation and attenuated cardiac diastolic dysfunction in rats with streptozotocin-induced diabetes. LY333531 suppressed the decreased expression of myocardial nitric oxide(NO), Cav-3, p-Akt, and p-eNOS, and also mitigated the augmentation of O_2^-, nitrotyrosine, Cav-1, and iNOS expression. In conclusion, hyperglycemia-induced PKCβ_2 activation requires caveolae, and is associated with reduced Cav-3 expression in the diabetic heart. Prevention of excessive PKCβ_2 activation attenuated cardiac diastolic dysfunction by restoring Cav-3 expression and subsequently rescuing Akt/eNOS/NO signaling.

Key words: PKC-β_2, caveolae, caveolin-3, diabetes

Introduction

Cardiovascular disease is the leading cause of diabetes-related death (1). While most diabetic heart failure etiology concerns coronary disease associated with atherosclerosis, a diabetes-associated cardiomyopathy has been reported in humans (2) and animal models of Type 1 (3) and Type 2 diabetes (4). Numerous studies by our group(5, 6) and others (7, 8) suggest the involvement of excess expression or activation of protein kinase C (PKC) β_2 in the development and progression of diabetic cardiomyopathy. Moreover, inhibition of PKCβ activation improves cardiac function in diabetic animals (9, 10). Despite these observations, the underlying mechanism by which PKCβ_2 activation exerts deleterious effects in the diabetic myocardium remains unclear.

PKCβ_1 and PKCβ_2 are two of classical isoforms (α, β, and γ) of PKC (11). Of the two isoforms, PKCβ_2 is preferentially overexpressed in the myocardium of patients (12) or animals (13) with diabetes. PKCβ_2 activation has been implicated in diabetes-associated abnormalities via inhibition of Akt-dependent endothelial nitric oxide (NO) synthase (eNOS) activity (14) and that restoration of Akt-eNOS-NO signaling has been shown to attenuate diabetic cardiomyopathy and myocardial dysfunction (15). Altered caveolae formation may potentially be the root cause of such inhibition. Caveolae, lipid rafts formed by small plasma membrane invaginations, serve as platforms modulating signal transduction pathways (e.g., PKC isoforms (16) via molecules docked with caveolin (Cav), a major constituent protein associated with caveolae. Of the three caveolin isoforms identified in mammalian caveolae, Cav-3 is mainly expressed in cardiac muscle, and is essential for proper formation of cardiomyocyte caveolae(17). Interestingly, in cardiomyocytes, eNOS localizes to

Cav-3 (18), permitting eNOS activation by cell surface receptors, and cellular surface NO release for intercellular signaling (18). Therefore, NO is an endogenous inhibitor of hypertrophic signaling (19), and Cav-3 is important for maintaining NO function. Additionally, Cav-3 has been demonstrated to inhibit growth signaling in the hearts of non-diabetic subjects (20). Thus, any alteration in Cav-3 expression in the diabetic condition may participate in the pathogenesis of diabetic cardiomyopathy, which is supported by findings that decreased cardiac Cav-3 expression is detected in rats with chronic streptozotocin (STZ)-induced diabetes (21, 22). In the present study, we hypothesize that PKCβ_2 activation induced by hyperglycemia promotes caveolae dysfunction with associated signaling abnormality. Our data suggests that excessive PKCβ_2 activation during diabetes reduces Cav-3 expression, with subsequent decreased Akt/eNOS signaling, which ultimately and negatively impact on cardiac remodeling and function.

RESEARCH DESIGN AND METHODS

Induction of diabetes and drug treatment

Male Sprague-Dawley rats (aged 8 weeks) weighing 260±10 g equilibrated to surroundings for three days before experiments. Diabetes was induced via single tail vein injection of STZ (60 mg/kg, Sigma, St. Louis, MO, USA) dissolved in citrate buffer (0.1 M, pH 4.5), while control rats were injected with an equal volume citrate buffer alone. One week after STZ injection, rats exhibiting hyperglycemia (blood glucose ≥16.7 mM) were considered diabetic, and were subjected to outlined experiments. One week after diabetes induction, rats were treated with vehicle or PKCβ inhibitor LY333531 (also named ruboxistaurin, a drug that has been approved by FDA for the prevention of vision loss in patients with diabetic retinopathy (23) by oral gavage for 4 weeks at dose of 1 mg/kg/day (demonstrated to adequately inhibit PKCβ activation in rat heart and vasculature (24, 25)). This model was chosen based on our most recent study (26) and the study of others (27) showing that STZ-diabetic rats developed cardiac dysfunciton 35 days after STZ-injection, with concomitant cardiomyocytes hypertrophy and cardiac fibrosis formation(26) , two major features of diabetic cardiomyopathy. After 4 weeks treatment, cardiac functions were determined, the rats were then deeply anesthetized with sodium pentobarbital (65 mg/kg), and hearts were rapidly excised either for cardiomyocyte isolation or frozen in liquid nitrogen for later analysis. Subgroups of control and untreated diabetic rats were terminated at 8 weeks of STZ-induced diabetes and heart tissue samples were processed to analyze changes of cardiac PKCβ_2 and Cav-3 at a relatively later phase of the disease. All experiments performed conformed to the Guide for the Care and Use of Laboratory Animals, published by the National Institutes of Health (NIH Publication No. 86-23, revised 1996) and were approved by the Institutional Animal Care and Use

Committee of Hong Kong University.

Echocardiography.

At the conclusion of 4 weeks treatments, transthoracic echocardiography was performed at experiment termination via a 17.5 MHz linear array transducer system (Vevo 770™, High Resolution Imaging System, Visual Sonics Inc., Canada) and left ventricular (LV) dimensions, LV diastolic and systolic function were assessed by M-mode and Doppler echocardiography as we previously described (26). LV internal dimensions at end systole (LVIDs) and diastole (LVIDd) were used to calculate fractional shorting (FS) by the following formula: FS(%) = (LVIDd-LVIDs)/LVIDd×100%. Left ventricular posterior wall dimensions at end diastole (LVPWd) and systole (LVPWs) were used to calculate fractional left ventricular posterior wall thickening (FLVPW) by the following formula: LVPW(%) = LVPWs-LVPWd/LVPWd×100%. The peak velocity of early (E) and late (A) diastolic filling were used to calculate the ratio of E and A (E/A). LV end-diastolic volume (LVVd) and end-systolic volume (LVVs) were used to calculate ejection fraction (EF) by the following formula: EF(%) = LVVd-LVVs/LVVd×100%. The heart rate (HR), systolic interventricular septal thickness (IVSs), diastolic interventricular septal thickness (IVSd), left ventricular isovolumic relaxation time (IVRT) and stroke volume (SV) were also monitored. All echocardiographically derived measures were obtained by averaging the readings of three consecutive beats.

Preparation of isolated rat ventricular cardiomyocytes

Calcium-tolerant cardiomyocytes were prepared from rat ventricles via a modified method as described (28). Cells isolated from a single rat heart were plated on

Matrigel-coated culture dishes and allowed to recover for 3 hours. Cultured ventricular cardiomyocytes were incubated in low glucose (5.5 mM), high glucose (25 mM), or mannitol/glucose (19.5 mMmannitol + 5.5 mM glucose) at 37 ℃in Medium 199 (Gibco, Grand Island, NY, USA)containing various treatments, and then snap frozen in liquid nitrogen for future analysis. LDH release (a measure of cell injury) in culture medium was detected via commercial LDH kit (Roche, Germany).

Immunoprecipitation

Isolated cardiomyocytes were homogenized in lysis buffer. 500 μg of cell extracts were subjected to immunoprecipitation with 2 μg of Cav-3 primary antibody in the presence of 20 μL protein A/G plus-agarose. After extensive PBS washes, theimmunoprecipitates were denatured with 1×SDS loading buffer, and subjected to analysis for PKCβ_2 expression by Western blot as described below.

Immunofluorescence

Isolated cardiomyocytes were plated on Matrigel pre-coated glass coverslips, incubated either in low or high glucose in Medium 199 for 36 hours, and fixed in ice-cold acetone for 5 minutes. The fixed cells were blocked in PBST with 10% goat serum and 1% BSA for 30 minutes, and further incubated with a mixture of mouse against rat Cav-3 antibody (1:50, Santa Cruz Biotechnology), and rabbit against rat PKCβ_2 antibody (1:100, Santa Cruz Biotechnology) in 1% BSA in PBST in a humidified chamber for 1 hour at room temperature. After three PBST washings, the cells were incubated for 1 hour with a mixture of Alexa Fluor® 488 goat anti-mouse IgG and Alexa Fluor® 594 goat anti-rabbit IgG (1:2000, Invitrogen, Carlsbad, CA). Cells were washed 3 times and prepared for confocal laser scanning microscopic imaging with mounting medium with

DAPI (Vector Laboratories, Inc., Burlingame, CA).

PKCβ$_2$ siRNA and Cav-3 siRNA studies in H9C2 cells

Embryonic rat cardiac H9C2 cells were maintained in DMEM medium containing 10% fetal bovine serum in a humidified atmosphere (5% CO_2) at 37 ℃. Commercial PKCβ$_2$ siRNA and Cav-3 siRNA (Santa Cruz Biotechnology) were utilized for inhibition of both PKCβ$_2$ and Cav-3 expression per manufacturer's protocol. After transfection with control, PKCβ$_2$ or Cav-3 siRNA, cells were incubated in either low or high glucose in DMEM medium for 36 hours, and snap frozen in liquid nitrogen.

Determination of myocardial levels of NO, O_2^-, and nitrotyrosine

Frozen heart tissues were pulverized separately with mortar and pestle in liquid nitrogen, homogenized in ice-cold PBS, and centrifuged at 3,000 g for 15 minutes at 4°C for supernatant collection. The supernatant protein concentration was determined via a Lowry assay kit (Bio-Rad, CA, USA). Concentrations of nitrites (NO_2^-) and nitrates (NO_3^-), the stable end products of nitric oxide (NO), were determined by the Griess reaction as previously described(29). NO levels were expressed as nmol/μg protein. Myocardial O_2^- production was determined via lucigeninchemiluminescence method (30, 31). The supernatant samples were loaded with dark-adapted lucigenin (5 μM), and read in 96-well microplates by luminometer (GloMax, Promega), with and without pretreatment with the NOS inhibitor L-NAME (100μM (15)) for 30 minutes at room temperature. Light emission, expressed as mean light units (MLU)/min/100 μg protein, was recorded for 5 minutes. Myocardial nitrotyrosine levels (μg/mg protein) in the collected supernatant were determined by chemiluminescence detection via the Nitrotyrosine Assay Kit per manufacturer's protocol (Millipore, USA).

Separation of cytosol and membrane fractions of heart tissues

In order to characterize subcellular distributions of targeted proteins, cytosol and membrane fractions of cardiac tissue lysate were separated by ultracentrifugation described previously (5). Cytosol and membrane fractions were denatured by 5×SDS loading buffer, and subjected to analysis for PKCβ_1 and PKCβ_2 expression by Western blot as described below.

Isolation of caveolin-rich fractions

Caveolae were isolated by discontinuous sucrose gradient centrifugation as described previously(22). Each heart sample gradient was separated into 12 fractions. Fractions 4-6 were considered the lipid raft fractions, and fractions 8-12 were considered the heavier fractions. Equal protein amounts were loaded for Western blot analysis.

Western blot analysis

Equal protein amounts from isolated cardiomyocytes, H9C2 cells, and rat heart homogenate were resolved by 7.5-12.5% SDS-PAGE and subsequently transferred to PVDF membrane for immunoblot analysis as described previously (32).

Statistical analysis

Densitometry was obtained by image analysis software (Bio-Rad). All values are presented as means ± S.E.M. Comparisons between multiple groups were made by one-way analysis of variance (ANOVA) followed by Tukey's test for multiple comparisons. Statistical analysis was performed by GraphPad Prism (GraphPad Software Inc., San Diego, CA, USA). P values less than 0.05 were considered

significant.

RESULTS

Expression and association of PKCβ$_2$ and Cav-3 in cardiomyocytes isolated from diabetic rats

We previously reported activation of the PKCβ$_{2,}$ but not PKCβ$_{1,}$ isoform in the diabetic heart (6). In the present study, we examined whether PKCβ$_2$ activation was associated with abnormal Cav-3 expression, a muscle-specific marker of caveolae(17). Diabetes moderately increased PKCβ$_2$ phosphorylation on thr-642 residue (data not shown), but the increase in phosphorylation of PKCβ$_2$ ~~on~~ was most profound at serine residue 660, without influencing total PKCβ$_2$, resulting in a markedly increased ratio of phosphorylated PKCβ$_2$/total PKCβ$_2$ (Figure 1A). Decreased Cav-3 expression was observed in cardiomyocytes isolated from 8-week diabetic rat hearts compared to age-matched control (Figure 1B). We next examined the relationship between Cav-3 and PKCβ$_2$ by immunoprecipitation experiments in isolated cardiomyocytes. While a small amount of PKCβ$_2$ remained constitutively associated with Cav-3 during basal conditions, the diabetic condition increased its association with Cav-3 (Figure 1C). To confirm our findings, we utilized confocal immunofluorescence staining. Limited PKCβ$_2$ was present during basal conditions in association with Cav-3 in the cell membrane (indicated by scant yellow punctate staining of the cell periphery); 36 hours of high-glucose (HG) stimulation significantly increased regions of co-localization between PKCβ$_2$ and Cav-3 compared to low-glucose (LG) stimulation (Figure 1D).

Effect of high-glucose on expression and association of p-PKCβ$_2$ and Cav-3 in

isolated cardiomyocytes over time

High-glucose conditions significantly increased the ratio of p-PKCβ_2/total PKCβ_2 (indicating PKCβ_2 activation) in cardiomyocytes within 1 hour, for up to 48 hours (Figure 2A). Peak increase in the ratio of p-PKCβ_2/total PKCβ_2 occurred after 12 hours HG exposure. The osmotic control mannitol exerted no effects upon p-PKCβ_2/total PKCβ_2 and Cav-3 expression (data not shown). In contrast to the quick increase of p-PKCβ_2/total PKCβ_2 early as 1 hour after HG exposure, Cav-3 expression did not significantly increase until 6-12 hours after HG exposure, reduced to basal levels within 24 hours, and significantly decreased 36-48 hours after initial HG exposure (Figure 2B). Cardiomyocyte LDH release significantly increased 24 hours after HG exposure, with rising tendency continuing 36-48 hours after initial HG exposure (Figure 2C).

Hyperglycemia-induced PKCβ_2 activation involves caveolae and is associated with reduced Cav-3 expression

We next investigate the interplay between PKCβ_2 activation and caveolae (and Cav-3) under hyperglycemic conditions. Given that PKCβ_1 activation induced by HG requires caveolae in primary mesangial cells (33), we determined whether caveolae are crucial in HG-induced PKCβ_2 activation in isolated cardiomyocytes from non-diabetic rats. As shown in Figure 3A, phosphorylation of PKCβ_2 induced by HG was prevented by either the selective PKCβ_2 inhibitor CGP-53353 (CGP, 1μM, from Sigma-Aldrch, USA, IC50 values are 0.41 μM and 3.8 μM respectively for PKCβ_2 and PKCβ_1) or methyl-β-cyclodextrin (CD, 50 μM, a disrupter of cholesterol-rich caveolae) (34). To determine whether Cav-3 is required for PKCβ_2 activation, we subjected H9C2 cells treated with rat-specific Cav3-siRNA to both low- and high-glucose conditions.

siRNA-mediated reduction of Cav-3 expression by ~60% (Figure 3B) prevented augmented phosphorylation of PKCβ_2 in HG conditions. No effects upon PKCβ_2 phosphorylation were observed in cells exposed to low glucose (LG) (Figure 3B). We also determined whether excessive PKCβ_2 activation induced by HG is associated with reduced Cav-3 expression. Selective inhibition of PKCβ_2 activation by CGP reversed the reduction of Cav-3 expression in primary cardiomyocytes exposed to HG (Figure 3C). Similarly, in H9C2 cells, knockdown of PKCβ_2 by siRNA reduced PKCβ_2 phosphorylation in cells incubated in LG and HG conditions (Figure 3D), and attenuated decreased Cav-3 expression in cells exposed to HG, with no impact upon Cav-3 expression in cells exposed to LG (Figure 3E).

Hyperglycemia-induced activation of PKCβ_2 is associated with caveolae-modulated Akt/eNOS signaling

Next, we investigate the impact of PKCβ_2 activation by HG, in the downstream signaling molecules Akt and eNOS, both modulated by caveolins(35). Cardiomyocytes incubated in HG exhibited decreased phosphorylation of Akt at Ser^{473} and eNOS at Ser^{1177}, and these decreases were reversed by CGP treatment (Figures 4A and B). Caveolar disruption by CD further exaggerated HG-mediated reduction of Akt phosphorylation (Figure 4A), but did not further exacerbate HG-induced reduction of p-eNOS expression (Figure 4B). However, CGP mediated restoration of eNOS phosphorylation in HG-treated cardiomyocytes was abolished during concomitant CD treatment (Figure 4B). To confirm the relative effects of PKCβ_2 and Cav-3 upon HG-mediated changes in p-AKT and p-eNOS, H9C2 cells were subject to both PKCβ_2 and Cav-3 knockdown by siRNA. PKCβ_2 knockdown significantly increased the phosphorylation of Akt and eNOS in HG-treated cells, effects which were not observed

in LG-treated cells (Figure 4C). Knockdown of Cav-3 resulted in further reduced expression of both p-Akt and p-eNOS in both LG and HG-treated cells (Figure 4D).

Inhibition of PKCβ$_2$ activation by LY333531 attenuates cardiac caveolar dysfunction in diabetic rats

To further investigate the role of PKCβ$_2$ activation in diabetes-induced abnormalities, we treated STZ-induced diabetic rats with the PKCβ inhibitor LY333531 for 4 weeks. PKCβ$_2$, but not PKCβ$_1$, isoform was excessively activated in the diabetic heart, as demonstrated by increased membrane translocation of PKCβ$_2$ but not PKCβ$_1$, a phenomenon inhibited by LY333531 (Figure 5A). PKCβ2-inhibitor LY333531 administration suppressed augmented whole-heart Cav-1 expression (Figure 5B), and prevented whole-heart decreased Cav-3 expression (Figure 5C). Caveolae fractions were isolated via discontinuous sucrose gradient centrifugation of whole cell lysates. Cav-1 was found predominantly in fractions 8-10, whereas Cav-3 was located within both lipid fractions (4-6) and heavier fractions (8-12). PKCβ$_2$ was predominantly co-expressed within Cav-3-rich fractions (Figure 5D). Densitometric analysis of all fractions (1-12) demonstrated that PKCβ2-inhibitor LY333531 significantly reduced augmented Cav-1 and PKCβ$_2$ expression, and suppressed decreased Cav-3 expression in diabetes (Figure 5E).

Inhibition of PKCβ$_2$ activation by LY333531 attenuates diastolic dysfunction in diabetic rats

At the end of the treatment period, untreated diabetic rats had significantly elevated blood glucose and reduced body weight and heart weight as compared to control rats, which were not altered by LY333531 treatment (Table 1). However, the ratio of

heart-weight to body-weight, an indirect index of myocardial hypertrophy, in the untreated diabetic rats was significantly higher than that in the control rats, which was significantly attenuated by LY333531 treatment (Table 1). Further, the left ventricular cardiomyocyte cross-sectional areas as assessed in H&E stained cardiac sections (methodology available at Online appendix) in the untreated diabetic rats was significantly bigger than that in the control rats and was significantly attenuated by LY333531 treatment (online appendix Figure 1), showing that LY333531 can attenuate cardiomyocyte hypertrophy in diabetes. We further determined rat cardiac function via echocardiography. As shown in table 1, no significant change in fractional shorting (FS), fractional left ventricular posterior wall thickening (FLVPW), and ejection fraction (EF) was observed among all experimental groups (although non-significant decreased values were recorded in the untreated diabetic group. Such data suggests preserved systolic function at 4-5 weeks in diabetic rats as used in our model. However, diastolic dysfunction was manifested. The heart rate (HR) and the ratio of peak velocity of early and late diastolic filling (E/A) was significantly decreased in diabetic rats as a consequence of significant reduction of E velocity and enhancement of A velocity that was concomitant with significant increase in left ventricular (LV) isovolumic relaxation time (IVRT) and reductions in LV end-diastolic volume (LVVd) and stroke volume (SV). Four weeks treatment with LY333531 restored the values of E/A, IVRT, LVVd and SV to levels that were comparable to that in the control rats but without significant effect upon HR.

LY333531 ameliorated diabetic-induced derangements of myocardial NO, O_2^- and nitrotyrosine content, and reverted changes in cardiac Akt, eNOS and iNOS

Diabetes is associated with decreased NO levels, and increased O_2^- and nitrotyrosine

production(15, 36), agents of oxidative and nitrative stress. To determine whether LY333531 conferred cardioprotection in part by reducing oxidative and nitrative stress in diabetes, the levels of NO, O_2^-, and nitrotyrosine in diabetic heart tissues were assessed. The diabetic condition significantly decreased NO levels (Figure 6A) and increased O_2^- (Figure 6B) and nitrotyrosine production (Figure 6C) in cardiac tissues. LY333531 suppressed all these derangements. Further studies revealed that the diabetes-induced augmented O_2^- levels could be blocked by the NOS inhibitor L-NAME (100 μM) (Figure 6B), suggesting a NOS-dependent mechanism for O_2^- accumulation. We next investigated related signaling molecules, including Akt, eNOS, and iNOS. The diabetic condition did not affect total cardiac Akt and eNOS expression, but significantly decreased p-Akt (Ser 473) and p-eNOS (Ser 1177) expression, both reversed by LY333531 (Figures 6D and E). Consistent with a recent study (37), our results demonstrated diabetes increased myocardial iNOS (an adverse marker mediating nitrative stress (24)), which was reversed by LY333531 (Figure 6F).

DISCUSSION

In the present study, we have demonstrated that hyperglycemia-induced cardiac PKCβ_2 activation requires caveolae. We provided evidence that excessive PKCβ_2 activation is associated with reduced Cav-3 expression, contributing to abnormal Akt/eNOS signaling during hyperglycemia. Inhibition of excessive activation of PKCβ_2 by compound LY333531 improves cardiac diastolic function, possibly via attenuation of caveolar dysfunction and rescuing Akt/eNOS/NO function in the diabetic heart. To our best knowledge, this is the first study examining the relationship between PKCβ_2 and Cav-3 in cardiomyocytes subjected to hyperglycemic conditions.

It is well-established that chronic hyperglycemia induces abnormal activation of PKC, which contributes to diabetic cardiovascular complications(38, 39). However, the PKC signaling pathway is complicated by numerous isoforms, each with varying cellular distribution and opposing function at times (40). The PKCβ_2 isoform is most frequently implicated in diabetic cardiovascular complications (5-8). Our current study further confirmed that PKCβ_2, but not PKCβ_1, is excessively activated in the diabetic heart. Although the precise mechanisms by which hyperglycemia induces PKCβ_2 activation in cardiomyocytes are not fully understood, evidence supports the vital role of caveolae (the specialized plasma membrane microdomains modulating signaling transduction pathways of molecules docked within them (17)) in hyperglycemia-induced PKCβ_2 activation. This is well supported by our immunoprecipitation and immunofluorescence studies demonstrating hyperglycemia increased the association and co-localization of PKCβ_2 and Cav-3. Caveolar disruption by methyl-β-cyclodextrin(34) suppressed hyperglycemia-induced PKCβ_2 activation in isolated cardiomyocytes. Cav-3 knockdown by siRNA prevented augmented PKCβ_2 phosphorylation in H9C2 cells exposed to high-glucose, suggesting that Cav-3 is

required specifically for hyperglycemia-induced PKCβ$_2$ activation in cardiomyocytes. Cav-3 is the predominant cardiomyocyte caveolin isoform essential for caveolar function. In the current study, we demonstrated that cardiomyocyte Cav-3 expression increased 6-12 hours after HG exposure but reduced to basal levels within 24 hours and progressively further reduced to lower than basal levels after 36 to 48 hours of HG exposure. The initial increase in Cav-3 expression after HG exposure observed in our study is an acute response to the calorie surplus similar to that reported by other researchers(41). The significant reduction of Cav-3 expression in cardiomyocytes after prolonged HG exposure is consistent with our results from the intact rats which showed that Cav-3 expression was decreased in isolated cardiomyocytes from rats of 8 and 5-week duration of diabetic condition. Loss of Cav-3 expression results in cardiomyopathy(42), and reduction in cardiac Cav3 protein expression is highly correlated with reduction in left ventricular fractional shortening in mice with constitutive overexpression of A1-adenosine receptor induced cardiac dilatation and dysfunction, and with makers of heart failure phenotype in humans (43). Our study results suggest excess PKCβ$_2$ activation contributes towards attenuated Cav-3 expression in the diabetic heart, as inhibition of PKCβ$_2$ activation by CGP53353 or siRNA-mediated PKCβ$_2$ expression knockdown prevented the decline of Cav-3 expression in cells exposed to HG. LY333531 treatment ameliorated diabetic heart caveolae dysfunction.

PKCβ$_2$ activation likely exerts adverse effects in the diabetic heart via alteration of the Akt/eNOS signaling pathway, which is modulated by caveolins(35). Although Cav-1 negatively regulates eNOS in cardiovascular tissues (44, 45), the co-localization of Cav-3 and eNOS may facilitate eNOS activation by both cell surface receptors and cellular surface NO release for intercellular signaling in cardiomyocytes(18). This is

supported by our findings that disruption of caveolae function by methyl-β-cyclodextrin or Cav-3 siRNA prevented Akt phosphorylation and suppressed eNOS phosphorylation in cardiomyocytes. Additionally, hyperglycemia decreased phosphorylated Akt and eNOS in both isolated cardiomyocytes and in diabetic heart tissues, leading to decreased myocardial NO levels, reduced Cav-3 levels, and increased Cav-1 cardiac levels. Inhibition of PKCβ_2 activation suppressed or abrogated these alterations. Therefore, inhibition of PKCβ_2 activation may rescue proper Akt/eNOS/NO signaling in the diabetic heart via caveolin regulation.

Previous studies have demonstrated involvement of increased iNOS expression with cardiovascular abnormalities in STZ-induced diabetic rats (24, 46). Our study confirms increased iNOS cardiac content in diabetic rats, an adverse mediator of nitrative stress (24), and increased nitrotyrosine was also demonstrated in diabetic heart tissue. The NOS inhibitor L-NAME blocked diabetes-induced augmentation of O_2^- levels, indicating eNOS uncoupling, which is in line with a recent study in STZ-induced diabetic mice (47). Furthermore, treatment of diabetic rats with LY333531 inhibited cardiac iNOS expression and reduced both nitrotyrosine and O_2^- production. Diabetes is associated with decreased NO levels and increased O_2^- and nitrotyrosine production (15, 36), which are implicated with oxidative/nitrative stress and eNOS uncoupling. Our study provides direct evidence showing that inhibition of PKCβ_2 activation can mitigate oxidative/nitrative stress and eNOS uncoupling.

Initial left ventricular diastolic dysfunction, reduced contractility, and prolonged diastole are the hallmarks of diabetic cardiomyopathy (48, 49). In the present study, diabetes significantly reduced E/A ratio that was concomitant with significantly increased IVRT and decreased LVVd and SV, but did not alter fractional shorting (FS), fractional left ventricular posterior wall thickening (FLVPW) or ejection fraction (EF).

Such data indicates that myocardial diastolic (but not systolic) dysfunction occurs in 45-week STZ-induced diabetic rats, which can be ameliorated by LY333531. Our findings are in general agreement with the findings of Mihm MJ et al (27) who conducted a series study in a similar STZ-diabetic rats and showed that diastolic dysfunction occurred early during the course of the disease which progressed to LV dilation reflected as increases in LVIDd and LVIDs with concomitant increase in LV luminal area and systolic dysfunction reflected as reduction in LV FS 35 days after STZ-injection and onward. It should be noted that the E/A ratio derived from the conventional Doppler echocardiography as used in our current study is not a load-independent parameter and may have inherent limitations, such as the peak E wave velocity can be highly dependent upon heart rate(27), while the heart rate in the diabetic rats was lower than that in the control group (Table 1). The newly developed Doppler tissue echocardiography (DTE) can acquire myocardial wall and mitral annular velocity online and the early diastolic annular velocity measured using DTE has been reported to be a preload independent index for evaluating LV diastolic function. A combination of DTE derived E'/A' ratio and the mitral inflow patterns (E/A ratio) obtained by conventional Doppler echocardiography in future studies should help to provide better estimations of diastolic dysfunction. However, the significant reduction of E/A ratio as a consequence of significant reduction of E velocity and significant enhancement of A velocity in combination with concomitant increase in IVRT and reductions in LVVD and SV in the diabetic group could jointly suggest diastolic dysfunction in the current study. LY333531 treatment in diabetic rats did not affect heart rate but corrected all the above changes, suggesting the LY333531 treatment prevented the development of diastolic dysfunction. Future functional study with cardiomyocytes isolated from various stages of diabetic rodents will help establish

the relative contribution of the slowing in cardiomyocyte relaxation time and left ventricular stiffness (due to fibrosis) to the development of diastolic dysfunction.

In summary, our study demonstrates that hyperglycemia-induced PKCβ_2 activation is associated with caveolar dysfunction, and consequently deranged Akt/eNOS signaling (Figure 7). Inhibition of PKCβ_2 activation attenuated cardiac diastolic dysfunction by restoring caveolin-3 expression and subsequently rescuing Akt/eNOS/NO signaling. PKCβ_2 blockade may therefore represent a novel therapeutic avenue in the treatment of diabetic cardiomyopathy.

ACKNOWLEDGMENTS

This study was supported by a grant from the National Natural Science Foundation of China (NSFC 81270899), and in part by a General Research Fund grant (784011M and 782910M) from the Research Grants Council of Hong Kong.

S.L. performed the study and wrote the manuscript. H.L., J.X., Y.L. and X.G. performed the study. J.W., K.N., W.L., X.M., B.R. contributed to data analysis and interpretation. M.I and Z.X reviewed/approved the research protocol. Z. X wrote the manuscript. Z. X takes full responsibility for the work as a whole, including the study design, access to data, and the decision to submit and publish the manuscript.

REFERENCES

1. Khavandi K, Khavandi A, Asghar O, Greenstein A, Withers S, Heagerty AM, Malik RA: Diabetic cardiomyopathy--a distinct disease? *Best Pract Res Clin Endocrinol Metab* 23: 347-360, 2009
2. Zarich SW,Nesto RW: Diabetic cardiomyopathy. *American heart journal* 118: 1000-1012, 1989
3. Kim DH, Kim YJ, Chang SA, Lee HW, Kim HN, Kim HK, Chang HJ, Sohn DW, Park YB: The protective effect of thalidomide on left ventricular function in a rat model of diabetic cardiomyopathy. *European journal of heart failure* 12: 1051-1060, 2010
4. Ni Q, Wang J, Li EQ, Zhao AB, Yu B, Wang M, Huang CR: Study on the protective effect of shengmai san (see text) on the myocardium in the type 2 diabetic cardiomyopathy model rat. *Journal of traditional Chinese medicine = Chung i tsa chih ying wen pan / sponsored by All-China Association of Traditional Chinese Medicine, Academy of Traditional Chinese Medicine* 31: 209-219, 2011
5. Xia Z, Kuo KH, Nagareddy PR, Wang F, Guo Z, Guo T, Jiang J, McNeill JH: N-acetylcysteine attenuates PKCbeta2 overexpression and myocardial hypertrophy in streptozotocin-induced diabetic rats. *Cardiovasc Res* 73: 770-782, 2007
6. Liu Y, Lei S, Gao X, Mao X, Wang T, Wong GT, Vanhoutte PM, Irwin MG, Xia Z: PKCbeta inhibition with ruboxistaurin reduces oxidative stress and attenuates left ventricular hypertrophy and dysfuntion in rats with streptozotocin-induced diabetes. *Clin Sci (Lond)* 122: 161-173, 2012
7. Gurusamy N, Watanabe K, Ma M, Zhang S, Muslin AJ, Kodama M, Aizawa Y: Inactivation of 14-3-3 protein exacerbates cardiac hypertrophy and fibrosis through enhanced expression of protein kinase C beta 2 in experimental diabetes. *Biol Pharm Bull* 28: 957-962, 2005
8. Way KJ, Isshiki K, Suzuma K, Yokota T, Zvagelsky D, Schoen FJ, Sandusky GE, Pechous PA, Vlahos CJ, Wakasaki H, King GL: Expression of connective tissue growth factor is increased in injured myocardium associated with protein kinase C beta2 activation and diabetes. *Diabetes* 51: 2709-2718, 2002
9. Wei L, Yin Z, Yuan Y, Hwang A, Lee A, Sun D, Li F, Di C, Zhang R, Cao F, Wang H: A PKC-beta inhibitor treatment reverses cardiac microvascular barrier dysfunction in diabetic rats. *Microvasc Res* 80: 158-165, 2010
10. Connelly KA, Kelly DJ, Zhang Y, Prior DL, Advani A, Cox AJ, Thai K, Krum H, Gilbert RE: Inhibition of protein kinase C-beta by ruboxistaurin preserves cardiac function and reduces extracellular matrix production in diabetic cardiomyopathy. *Circ Heart Fail* 2: 129-137, 2009
11. Clarke M,Dodson PM: PKC inhibition and diabetic microvascular complications. *Best practice & research. Clinical endocrinology &*

metabolism 21: 573-586, 2007

12. Simpson PC: Beta-protein kinase C and hypertrophic signaling in human heart failure. *Circulation* 99: 334-337, 1999
13. Connelly KA, Kelly DJ, Zhang Y, Prior DL, Advani A, Cox AJ, Thai K, Krum H, Gilbert RE: Inhibition of protein kinase C-beta by ruboxistaurin preserves cardiac function and reduces extracellular matrix production in diabetic cardiomyopathy. *Circulation. Heart failure* 2: 129-137, 2009
14. Naruse K, Rask-Madsen C, Takahara N, Ha SW, Suzuma K, Way KJ, Jacobs JR, Clermont AC, Ueki K, Ohshiro Y, Zhang J, Goldfine AB, King GL: Activation of vascular protein kinase C-beta inhibits Akt-dependent endothelial nitric oxide synthase function in obesity-associated insulin resistance. *Diabetes* 55: 691-698, 2006
15. Ren J, Duan J, Thomas DP, Yang X, Sreejayan N, Sowers JR, Leri A, Kajstura J, Gao F, Anversa P: IGF-I alleviates diabetes-induced RhoA activation, eNOS uncoupling, and myocardial dysfunction. *Am J Physiol Regul Integr Comp Physiol* 294: R793-802, 2008
16. Rybin VO, Xu X, Steinberg SF: Activated protein kinase C isoforms target to cardiomyocyte caveolae : stimulation of local protein phosphorylation. *Circ Res* 84: 980-988, 1999
17. Panneerselvam M, Patel HH, Roth DM: Caveolins and heart diseases. *Adv Exp Med Biol* 729: 145-156, 2012
18. Feron O,Balligand JL: Caveolins and the regulation of endothelial nitric oxide synthase in the heart. *Cardiovasc Res* 69: 788-797, 2006
19. Kempf T,Wollert KC: Nitric oxide and the enigma of cardiac hypertrophy. *Bioessays* 26: 608-615, 2004
20. Fujita T, Otsu K, Oshikawa J, Hori H, Kitamura H, Ito T, Umemura S, Minamisawa S, Ishikawa Y: Caveolin-3 inhibits growth signal in cardiac myoblasts in a Ca2+-dependent manner. *J Cell Mol Med* 10: 216-224, 2006
21. Penumathsa SV, Thirunavukkarasu M, Zhan L, Maulik G, Menon VP, Bagchi D, Maulik N: Resveratrol enhances GLUT-4 translocation to the caveolar lipid raft fractions through AMPK/Akt/eNOS signalling pathway in diabetic myocardium. *J Cell Mol Med* 12: 2350-2361, 2008
22. Penumathsa SV, Thirunavukkarasu M, Samuel SM, Zhan L, Maulik G, Bagchi M, Bagchi D, Maulik N: Niacin bound chromium treatment induces myocardial Glut-4 translocation and caveolar interaction via Akt, AMPK and eNOS phosphorylation in streptozotocin induced diabetic rats after ischemia-reperfusion injury. *Biochim Biophys Acta* 1792: 39-48, 2009
23. Galvez MI: Protein kinase C inhibitors in the treatment of diabetic retinopathy. Review. *Curr Pharm Biotechnol* 12: 386-391, 2011
24. Nagareddy PR, Soliman H, Lin G, Rajput PS, Kumar U, McNeill JH, MacLeod KM: Selective inhibition of protein kinase C beta(2) attenuates inducible nitric oxide synthase-mediated cardiovascular abnormalities in

streptozotocin-induced diabetic rats. *Diabetes* 58: 2355-2364, 2009

25. Ishii H, Jirousek MR, Koya D, Takagi C, Xia P, Clermont A, Bursell SE, Kern TS, Ballas LM, Heath WF, Stramm LE, Feener EP, King GL: Amelioration of vascular dysfunctions in diabetic rats by an oral PKC beta inhibitor. *Science* 272: 728-731, 1996
26. Gao X, Xu Y, Xu B, Liu Y, Cai J, Liu HM, Lei S, Zhong YQ, Irwin MG, Xia Z: Allopurinol attenuates left ventricular dysfunction in rats with early stage of streptozotocin-induced diabetes. *Diabetes Metab Res Rev*, 2012
27. Mihm MJ, Seifert JL, Coyle CM, Bauer JA: Diabetes related cardiomyopathy time dependent echocardiographic evaluation in an experimental rat model. *Life Sci* 69: 527-542, 2001
28. Wang T, Qiao S, Lei S, Liu Y, Ng KF, Xu A, Lam KS, Irwin MG, Xia Z: N-acetylcysteine and allopurinol synergistically enhance cardiac adiponectin content and reduce myocardial reperfusion injury in diabetic rats. *PLoS One* 6: e23967, 2011
29. Luo T, Xia Z, Ansley DM, Ouyang J, Granville DJ, Li Y, Xia ZY, Zhou QS, Liu XY: Propofol dose-dependently reduces tumor necrosis factor-alpha-Induced human umbilical vein endothelial cell apoptosis: effects on Bcl-2 and Bax expression and nitric oxide generation. *Anesth Analg* 100: 1653-1659, 2005
30. Li YL, Gao L, Zucker IH, Schultz HD: NADPH oxidase-derived superoxide anion mediates angiotensin II-enhanced carotid body chemoreceptor sensitivity in heart failure rabbits. *Cardiovasc Res* 75: 546-554, 2007
31. Li JM,Shah AM: Mechanism of endothelial cell NADPH oxidase activation by angiotensin II. Role of the p47phox subunit. *J Biol Chem* 278: 12094-12100, 2003
32. Lei S, Liu Y, Liu H, Yu H, Wang H, Xia Z: Effects of N-acetylcysteine on nicotinamide dinucleotide phosphate oxidase activation and antioxidant status in heart, lung, liver and kidney in streptozotocin-induced diabetic rats. *Yonsei Med J* 53: 294-303, 2012
33. Zhang Y, Peng F, Gao B, Ingram AJ, Krepinsky JC: High glucose-induced RhoA activation requires caveolae and PKCbeta1-mediated ROS generation. *Am J Physiol Renal Physiol* 302: F159-172, 2012
34. Christian AE, Haynes MP, Phillips MC, Rothblat GH: Use of cyclodextrins for manipulating cellular cholesterol content. *J Lipid Res* 38: 2264-2272, 1997
35. Krajewska WM,Maslowska I: Caveolins: structure and function in signal transduction. *Cell Mol Biol Lett* 9: 195-220, 2004
36. Jin HR, Kim WJ, Song JS, Piao S, Choi MJ, Tumurbaatar M, Shin SH, Yin GN, Koh GY, Ryu JK, Suh JK: Intracavernous delivery of a designed angiopoietin-1 variant rescues erectile function by enhancing endothelial regeneration in the streptozotocin-induced diabetic mouse. *Diabetes* 60:

969-980, 2011
37. Cheng YS, Dai DZ, Ji H, Zhang Q, Dai Y: Sildenafil and FDP-Sr attenuate diabetic cardiomyopathy by suppressing abnormal expression of myocardial CASQ2, FKBP12.6, and SERCA2a in rats. *Acta Pharmacol Sin* 32: 441-448, 2011
38. Geraldes P,King GL: Activation of protein kinase C isoforms and its impact on diabetic complications. *Circ Res* 106: 1319-1331, 2010
39. Danis RP,Sheetz MJ: Ruboxistaurin: PKC-beta inhibition for complications of diabetes. *Expert Opin Pharmacother* 10: 2913-2925, 2009
40. Mellor H,Parker PJ: The extended protein kinase C superfamily. *Biochem J* 332 (Pt 2): 281-292, 1998
41. Gomez-Ruiz A, de Miguel C, Campion J, Martinez JA, Milagro FI: Time-dependent regulation of muscle caveolin activation and insulin signalling in response to high-fat diet. *FEBS letters* 583: 3259-3264, 2009
42. Woodman SE, Park DS, Cohen AW, Cheung MW, Chandra M, Shirani J, Tang B, Jelicks LA, Kitsis RN, Christ GJ, Factor SM, Tanowitz HB, Lisanti MP: Caveolin-3 knock-out mice develop a progressive cardiomyopathy and show hyperactivation of the p42/44 MAPK cascade. *J Biol Chem* 277: 38988-38997, 2002
43. Feiner EC, Chung P, Jasmin JF, Zhang J, Whitaker-Menezes D, Myers V, Song J, Feldman EW, Funakoshi H, Degeorge BR, Jr., Yelamarty RV, Koch WJ, Lisanti MP, McTiernan CF, Cheung JY, Bristow MR, Chan TO, Feldman AM: Left ventricular dysfunction in murine models of heart failure and in failing human heart is associated with a selective decrease in the expression of caveolin-3. *J Card Fail* 17: 253-263, 2011
44. Elcioglu KH, Kabasakal L, Cetinel S, Conturk G, Sezen SF, Ayanoglu-Dulger G: Changes in caveolin-1 expression and vasoreactivity in the aorta and corpus cavernosum of fructose and streptozotocin-induced diabetic rats. *Eur J Pharmacol* 642: 113-120, 2010
45. Lam TY, Seto SW, Lau YM, Au LS, Kwan YW, Ngai SM, Tsui KW: Impairment of the vascular relaxation and differential expression of caveolin-1 of the aorta of diabetic +db/+db mice. *Eur J Pharmacol* 546: 134-141, 2006
46. Nagareddy PR, Xia Z, McNeill JH, MacLeod KM: Increased expression of iNOS is associated with endothelial dysfunction and impaired pressor responsiveness in streptozotocin-induced diabetes. *Am J Physiol Heart Circ Physiol* 289: H2144-2152, 2005
47. Roe ND, Thomas DP, Ren J: Inhibition of NADPH oxidase alleviates experimental diabetes-induced myocardial contractile dysfunction. *Diabetes Obes Metab* 13: 465-473, 2011
48. Norby FL, Aberle NS, 2nd, Kajstura J, Anversa P, Ren J: Transgenic overexpression of insulin-like growth factor I prevents streptozotocin-induced cardiac contractile dysfunction and

beta-adrenergic response in ventricular myocytes. *J Endocrinol* 180: 175-182, 2004

49. Palmieri V, Capaldo B, Russo C, Iaccarino M, Pezzullo S, Quintavalle G, Di Minno G, Riccardi G, Celentano A: Uncomplicated type 1 diabetes and preclinical left ventricular myocardial dysfunction: insights from echocardiography and exercise cardiac performance evaluation. *Diabetes Res Clin Pract* 79: 262-268, 2008

Table 1

General characteristics and echocardiographic assessment of left ventricle dimensions and functions in rats

	C	D	D+LY
Blood glucose (mM)	6.26±0.53	28.24±4.64**	27.32±3.43**
Body weight (g)	490.1±14.3	295.4±28.8*	371.1±17.4*
Heart weight (g)	1.66±0.15	1.25±0.18*	1.31±0.16*
Heart weight/bodyweight (mg/g)	3.39±0.07	4.23±0.06*	3.53±0.08#
HR (bpm)	332±7.8	270±10.8*	286±9.2*
LVIDs (mm)	4.75±0.43	4.68±0.41	4.74±0.49
LVIDd (mm)	8.29±0.53	7.61±0.62	8.13±0.49
FS (%)	42.70±4.13	38.50±5.42	41.53±3.84
IVSs (mm)	2.23±0.16	2.28±0.07	2.27±0.13
IVSd (mm)	1.72±0.05	1.75±0.05	1.73±0.06
LVPWs (mm)	2.90±0.08	2.92±0.07	2.91±0.06
LVPWd (mm)	1.85±0.06	1.91±0.09	1.87±0.08
LVPW (%)	56.76±7.50	52.88±10.03	55.61±4.81
LVVs (μL)	107.6±15.8	109.8±13.7	114.5±11.9
LVVd (μL)	378.7±25.6	315.4±21.8*	380.4±19.7#
EF (%)	71.6±4.7	65.2±5.7	69.9±3.9
IVRT (ms)	21.75±1.25	27.83±1.80*	20.63±1.38#
E Velocity (cm/s)	1340.9±44.6	1217.8±33.7*	1331.0±40.8#
A Velocity (cm/s)	890.1±37.1	1023.4±34.7*	917.9±28.9#
E/A	1.49±0.09	1.19±0.05*	1.45±0.085#
SV (μL)	285.7±19.1	230.8±17.9*	279.4±20.8#

Control or STZ-induced diabetic rats were either untreated or treated with PKCβ inhibitor LY333531 (LY, 1 mg/kg/day) by oral gavage for four weeks. HR, heart rate; LV, left ventricle; LVIDs, LV internal systolic diameter; LVIDd, LV internal diastolic diameter; FS, fractional shortening; IVSs, systolic interventricular septal thickness;

IVSd, diastolic interventricular septal thickness; LVPWs, LV systolic posterior wall thickness; LVPWd, LV diastolic posterior wall thickness; LVVs, LV end-systolic volume; LVVd, LV end-diastolic volume; EF, ejection fraction; IVRT, isovolumetric relaxation time; SV, stroke volume. All the results are expressed as means ± S.E.M., n = 8, control (C), diabetes (D), LY333531 (LY). $^{*}P < 0.05$, $^{**}P < 0.01$ vs. C; $^{\#}P < 0.05$ vs. D.

Titles and legends to figures

Figure 1. Expression of PKCβ$_2$ and Cav-3 in cardiomyocytes isolated from control and STZ-induced diabetic rats (8-weeks). (A) Representative Western blot demonstrating p-PKCβ$_2$ (Ser 660) and total-PKCβ$_2$ expression. (B) Representative Western blot demonstrating Cav-3 expression with GAPDH as loading control. (C) Cell lysates containing equal amounts of total protein were subjected to immunoprecipitation with anti-Cav-3 antibody, and analyzed by immunoblot with PKCβ$_2$ and Cav-3 antibody. All results expressed as means ± S.E.M., n=6-8 per group, $^{*}P<0.05$ vs. control. (D) Confocal laser microscopic image of adult rat cardiomyocytes in response to high glucose. Isolated cardiomyocytes from non-diabetic rats were incubated with low or high glucose for 36 hours, and underwent standard immunofluorescent staining with PKCβ$_2$ and Cav-3 antibodies (see Methods).

Figure 2. Effects of high glucose upon p-PKCβ$_2$ (Ser-660) and Cav-3 expression and LDH release in cultured cardiomyocytes over time. Representative Western blot of p-PKCβ$_2$ (Ser 660) expression in comparison with (A) total-PKCβ$_2$ and (B) Cav-3 expression with GAPDH as loading control. (C) Effects of high glucose upon LDH release. $^{*}P<0.05$ vs. control (time "0") group.

Figure 3. Expression of p-PKCβ$_2$ and Cav-3 in cultured cardiomyocytes and H9C2 cells following various treatments in low (5.5 mM) or high (25 mM) glucose conditions for 36 hours. (A) Representative Western blot demonstrating p-PKCβ$_2$ (Ser 660) in comparison to total-PKCβ$_2$ in cardiomyocytes exposed to high glucose in the presence

of a selective PKCβ_2 inhibitor CGP-53353 (CGP, 1μM) or methyl-β-cyclodextrin (CD, 10 μM). (B) Representative Western blot demonstrating p-PKCβ_2 and Cav-3 expression in H9C2 cells transfected with Cav-3 siRNA, exposed to low or high glucose. (C) Representative Western blot demonstrating Cav-3 expression in cultured cardiomyocytes exposed to high glucose in the presence of CGP (1μM). Representative Western blot demonstrating (D) p-PKCβ_2, total PKCβ_2 expression, and (D) Cav-3 expression in H9C2 cells transfected with PKC$\beta_2$siRNA in low or high glucose conditions. GADPH served as loading control. All results are expressed as means ± S.E.M., n=7, $^{*}P<0.05$ vs. all other groups, $^{\#}P<0.05$ vs. control-siRNA treated groups.

Figure 4. Expression of p-Akt (Ser 473) and p-eNOS (Ser 1177) in cultured cardiomyocytes and H9C2 cells in various treatments in low (5.5 mM) or high glucose (25 mM) conditions for 36 hours. (A) Representative Western blot demonstrating p-Akt in comparison to total Akt, and (B) p-eNOS in comparison with total eNOS in cardiomyocytes exposed to high glucose in the presence of a selective PKCβ_2 inhibitor CGP-53353 (CGP, 1μM), methyl-β-cyclodextrin (CD, 10 μM), or CGP+CD combination. Representative Western blot demonstrating p-Akt and p-eNOS expression in H9C2 cells transfected with (C) PKC$\beta_2$siRNA or (D) Cav-3 siRNA in low or high glucose conditions. GAPDH served as loading control. All results are expressed as means ± S.E.M., n=7, $^{*}P<0.05$ vs. all other groups, $^{\#}P<0.05$ vs. control-siRNA treated groups.

Figure 5. Effects of PKCβ inhibitor (LY333531) treatment upon subcellular distributions of PKCβ_1 and PKCβ_2, and expression levels of Cav-1 and Cav-3 in total heart preparations and various isolated cellular fractions. Control (C) or STZ-induced

diabetic rats were treated with PKCβ inhibitor LY333531 (1 mg/kg/day, D+LY) or control (D) by oral gavage for four weeks. (A) Representative Western blot demonstrating $PKC\beta_1$ and $PKC\beta_2$ protein expression. GAPDH and Na-K-ATPase served as loading controls in cytosol fractions or membrane fractions respectively. (Bottom graph) Membrane:cytosol ratio as indexes of PKCβ isoform translocation. Representative Western blot demonstrating (B) Cav-1 and (C) Cav-3 content in total heart preparations. (D) Sucrose gradient centrifugation isolated caveolae-enriched fractions. Aliquots containing equal amounts of protein or a volume equal to that of the fraction with the least detectable amount of protein for "protein-free" fractions (1 and 2), and unfractionated samples (UF) were probed for Cav-1, Cav-3, and $PKC\beta_2$immunoreactivity. (E) Cav-1 and Cav-3 and $PKC\beta_2$ expression in all the fractions (1-12) were calculated by relative densitometric values, and expressed as percentage of control. All results expressed as means ± S.E.M., n=7, $^{*}P<0.05$ vs. all other groups.

Figure 6. Effects of PKCβ inhibitor (LY333531) treatment upon the levels of NO, O_2^-, nitrotyrosine, and protein expression of p-Akt, p-eNOS, and iNOS in diabetic myocardium. Control (C) or STZ-induced diabetic rats were treated with PKCβ inhibitor LY333531 (1 mg/kg/day, D+LY) or control (D) by oral gavage for four weeks. Effects of LY333531 upon (A) myocardial NO levels, (B) O_2^- levels in the absence and presence of L-NAME, and (C) nitrotyrosine levels; Representative Western blot of (D) p-Akt compared to total Akt, (E) p-eNOS compared to total eNOS, and (F) iNOS with GAPDH as loading control. All results expressed as means ± S.E.M., n=7, $^{*}P<0.05$ vs. all other groups.

Figure 7. Schematic depicting hyperglycemia-induced PKCβ2 activation effects upon Cav-3-modulated Akt/eNOS signaling pathway.Cardiomyocytecaveolae are required for hyperglycemia-induced $PKC\beta_2$ activation (translocation from cytosol to caveolae membrane). Excessive $PKC\beta_2$activation decreased cav-3 expression, impairing the Akt/eNOS signaling pathway. Solid arrows depict stimulation, while transverse "T" shape indicates inhibition.

Hyperglycemia-induced PKCβ_2 Activation Induces Diastolic Cardiac Dysfunction in Diabetic Rats by Impairing Caveolin-3 Expression and Akt/eNOS Signaling

Shaoqing Lei[1], Haobo Li[1], Jinjin Xu[1], Yanan Liu[1], Xia Gao[1], Junwen Wang [2;3], Kwok F.J. Ng [1;3], Wayne Bond Lau[4], Xin-liang Ma[4], Brian Rodrigues[5], Michael G. Irwin[1;3#]and Zhengyuan Xia[1;3#]

[1]Department of Anesthesiology, [2]Department of Biochemistry, The University of Hong Kong, Hong Kong SAR, China; [3]Shenzhen Institute of Research & Innovation, The University of Hong Kong, Shenzhen, China; [4]Department of Emergency Medicine, Thomas Jefferson University, 1020 Sansom Street, Philadelphia, PA 19107, USA; [5]Faculty of Pharmaceutical Sciences, The University of British Columbia, Vancouver, BC, Canada

Running title: Hyperglycemia induces protein kinase C (PKC) β_2 activation

Words count: ~~3500~~ 4000

Number of figures: ~~8~~7

#MG Irwin and Z Xia share senior authorship

Address correspondence to:

Dr. Zhengyuan Xia

Department of Anesthesiology, University of Hong Kong, Hong Kong SAR, China

Tel: (852) 28199794; Fax: (852) 2819-9791

E-mail: zyxia@hku.hk

Abstract

~~Hyperglycemia induced p~~ Protein kinase C (PKC) β_2 ~~activation~~ is preferably overexpressed in the diabetic myocardium, which induces cardiomyocyte hypertrophy and contributes to diabetic cardiomyopathy, but the underlying mechanisms ~~is~~ are incompletely understood. Caveolae are critical in signal transduction of PKC isoforms in cardiomyocytes. Caveolin (Cav)-3 ~~(Cav-3)~~, the cardiomyocyte-specific caveolar structural protein isoform, is decreased in the diabetic heart. The current study determined whether PKCβ_2 activation affects caveolae and Cav-3 expression. Immunoprecipitation and immunofluorescence analysis revealed that ~~hyperglycemia~~ high glucose (HG) increased the association and co-localization of PKCβ_2 and Cav-3 in isolated cardiomyocytes. Disruption of caveolae by methyl-β-cyclodextrin ~~(CD)~~ or Cav-3 siRNA transfection prevented ~~hyperglycemia~~ HG-induced PKCβ_2 phosphorylation. Inhibition of PKCβ_2 activation by compound CGP53353 or knockdown of PKCβ_2 expression via siRNA attenuated the reductions of Cav-3 expression and Akt/eNOS phosphorylation in cardiomyocytes exposed to ~~high glucose~~ HG. ~~Inhibition of PKCβ2 activation with~~ LY333531 treatment (for a duration of 4 weeks) prevented excessive PKCβ_2 activation and attenuated cardiac diastolic dysfunction in rats with streptozotocin-induced diabetes. LY333531 suppressed the decreased expression of myocardial nitric oxide (NO), Cav-3, p-Akt, and p-eNOS, and also mitigated the augmentation of O_2^-, nitrotyrosine, ~~caveolin-1~~ Cav-1, and iNOS expression. In conclusion, hyperglycemia-induced PKCβ_2 activation requires caveolae, and is associated with reduced Cav-3 expression in the diabetic heart. ~~Inhibition~~ Prevention of excessive PKCβ_2 activation attenuated cardiac diastolic dysfunction by restoring Cav-3 expression and subsequently rescuing Akt/eNOS/NO signaling.

Key words: PKC-β_2, caveolae, caveolin-3, diabetes

Introduction

Cardiovascular disease is the leading cause of diabetes-related death (1). While most diabetic heart failure etiology concerns coronary disease associated with atherosclerosis, a diabetes-associated cardiomyopathy has been reported in humans (2) and animal models of Type 1 (3) and Type 2 diabetes (4). Numerous studies by our group(5, 6) and others (7, 8) suggest the involvement of excess expression or activation of protein kinase C (PKC) β_2 in the development and progression of diabetic cardiomyopathy. Moreover, inhibition of PKCβ activation improves cardiac function in diabetic animals (9, 10). Despite these observations, the underlying mechanism by which PKCβ_2 activation exerts deleterious effects in the diabetic myocardium remains unclear.

PKCβ_1 and PKCβ_2 are two of classical isoforms (α, β, and γ) of PKC (11). Of the two isoforms, PKCβ_2 is preferentially overexpressed in the myocardium of patients (12) or animals (13) with diabetes. PKCβ_2 activation has been implicated in diabetes-associated abnormalities via inhibition of Akt-dependent endothelial nitric oxide (NO) synthase (eNOS) activity (14) and that restoration of Akt-eNOS-NO signaling has been shown to attenuate diabetic cardiomyopathy and myocardial dysfunction (15). Altered caveolae formation may potentially be the root cause of such inhibition. Caveolae, lipid rafts formed by small plasma membrane invaginations, serve as platforms modulating signal transduction pathways (e.g., PKC isoforms (16) via molecules docked with caveolin (Cav), a major constituent protein associated with caveolae. Of the three caveolin isoforms identified in mammalian caveolae, Cav-3 is mainly expressed in cardiac muscle, and is essential for proper formation of cardiomyocyte_caveolae(17). Interestingly, in cardiomyocytes, eNOS localizes to

Cav-3 (18), permitting eNOS activation by cell surface receptors, and cellular surface NO release for intercellular signaling (18). Therefore, NO is an endogenous inhibitor of hypertrophic signaling (19), and Cav-3 is important for maintaining NO function. Additionally, Cav-3 has been demonstrated to inhibit growth signaling in the hearts of non-diabetic subjects (20). Thus, any alteration in Cav-3 expression in the diabetic condition may participate in the pathogenesis of diabetic cardiomyopathy, which is supported by findings that decreased cardiac Cav-3 expression is detected in rats with chronic streptozotocin (STZ)-induced diabetes (21, 22). In the present study, we hypothesize that PKCβ_2 activation induced by hyperglycemia promotes caveolae dysfunction with associated signaling abnormality. Our data suggests that excessive PKCβ_2 activation during diabetes reduces Cav-3 expression, with subsequent decreased Akt/eNOS signaling, which ultimately and negatively impact on cardiac remodeling and function.

RESEARCH DESIGN AND METHODS

Induction of diabetes and drug treatment

Male Sprague-Dawley rats (aged 8 weeks) weighing ~~between~~ 260±10 g equilibrated to surroundings for three days before experiments. Diabetes was induced via single tail vein injection of STZ (60 mg/kg, Sigma, St. Louis, MO, USA) dissolved in citrate buffer (0.1 M, pH 4.5), while control rats were injected with an equal volume citrate buffer alone. One week after STZ injection, rats exhibiting hyperglycemia (blood glucose ≥16.7 mM) were considered diabetic, and were subjected to outlined experiments. One week after diabetes induction, rats were treated with vehicle or PKCβ inhibitor LY333531 (also named ruboxistaurin, a drug that has been approved by FDA for the prevention of vision loss in patients with diabetic retinopathy (23) by oral gavage for 4 weeks at dose of 1 mg/kg/day (demonstrated to adequately inhibit PKCβ activation in rat heart and vasculature (24, 25)). This model was chosen based on our most recent study (26) and the study of others (27) showing that STZ-diabetic rats developed cardiac dysfunciton 35 days after STZ-injection, with concomitant cardiomyocytes hypertrophy and cardiac fibrosis formation(26) , two major features of diabetic cardiomyopathy. After 4 weeks treatment, ~~Following determination of~~ cardiac functions were determined, the rats were then deeply anesthetized with sodium pentobarbital (65 mg/kg), and hearts were rapidly excised either for cardiomyocyte isolation or frozen in liquid nitrogen for later analysis. Subgroups of control and untreated diabetic rats were terminated at 8 weeks of STZ-induced diabetes and heart tissue samples were processed to analyze changes of cardiac $PKC\beta_2$ and Cav-3 at a relatively later phase of the disease. All experiments performed conformed to the Guide for the Care and Use of Laboratory Animals, published by the National Institutes of Health (NIH Publication No. 86-23, revised 1996) and were

approved by the Institutional Animal Care and Use Committee of Hong Kong University.

Echocardiography.

At the conclusion of 4 weeks treatments, transthoracic echocardiography was performed at experiment termination via a 17.5 MHz linear array transducer system (Vevo 770™, High Resolution Imaging System, Visual Sonics Inc., Canada) and left ventricular (LV) dimensions, LV diastolic and systolic function were assessed by M-mode and Doppler echocardiography as we previously described (26). ~~Rats were lightly anesthetized by inhaled 2-3% isopentane for recording duration. Left ventricular~~ LV internal dimensions at end systole (LVIDs) and diastole (LVIDd) were used to calculate fractional shorting (FS) by the following formula: FS(%) = (LVIDd-LVIDs)/LVIDd×100%. Left ventricular posterior wall dimensions at end diastole (LVPWd) and systole (LVPWs) were used to calculate fractional left ventricular posterior wall thickening (FLVPW) by the following formula: LVPW(%) = LVPWs-LVPWd/LVPWd×100%. The peak velocity of early (E) and late (A) diastolic filling were used to calculate the ratio of E and A (E/A). LV end-diastolic volume (LVVd) and end-systolic volume (LVVs) were used to calculate ejection fraction (EF) by the following formula: EF(%) = LVVd-LVVs/LVVd×100%. The heart rate (HR), systolic interventricular septal thickness (IVSs), diastolic interventricular septal thickness (IVSd), left ventricular isovolumic relaxation time (IVRT) and stroke volume (SV) were also monitored. All echocardiographically derived measures were obtained by averaging the readings of three consecutive beats.

Preparation of isolated rat ventricular cardiomyocytes

Calcium-tolerant cardiomyocytes were prepared from rat ventricles via a modified method as described (28). Cells isolated from a single rat heart were plated on Matrigel-coated culture dishes and allowed to recover for 3 hours. Cultured ventricular cardiomyocytes ~~cells~~ were incubated in low glucose (5.5 mM), high glucose (25 mM), or mannitol/glucose (19.5 mMmannitol + 5.5 mM glucose) at 37 ℃ in Medium 199 (Gibco, Grand Island, NY, USA)containing various treatments, and then snap frozen in liquid nitrogen for future analysis. LDH release (a measure of cell injury) in culture medium was detected via commercial LDH kit (Roche, Germany).

Immunoprecipitation

Isolated cardiomyocytes were homogenized in lysis buffer. 500 μg of cell extracts were subjected to immunoprecipitation with 2 μg of Cav-3 primary antibody in the presence of 20 μL protein A/G plus-agarose. After extensive PBS washes, theimmunoprecipitates were denatured with 1×SDS loading buffer, and subjected to analysis for PKCβ_2 expression by Western blot as described below.

Immunofluorescence

Isolated cardiomyocytes were plated on Matrigel pre-coated glass coverslips, incubated either in low or high glucose in Medium 199 for 36 hours, and fixed in ice-cold acetone for 5 minutes. The fixed cells were blocked in PBST with 10% goat serum and 1% BSA for 30 minutes, and further incubated with a mixture of mouse against rat Cav-3 antibody (1:50, Santa Cruz Biotechnology), and rabbit against rat PKCβ_2 antibody (1:100, Santa Cruz Biotechnology) in 1% BSA in PBST in a humidified chamber for 1 hour at room temperature. After three PBST washings, the cells were incubated for 1 hour with a mixture of Alexa Fluor® 488 goat anti-mouse

IgG and Alexa Fluor® 594 goat anti-rabbit IgG (1:2000, Invitrogen, Carlsbad, CA). Cells were washed 3 times and prepared for confocal laser scanning microscopic imaging with mounting medium with DAPI (Vector Laboratories, Inc., Burlingame, CA).

PKCβ$_2$ siRNA and Cav-3 siRNA studies in H9C2 cells

Embryonic rat cardiac H9C2 cells were maintained in DMEM medium containing 10% fetal bovine serum in a humidified atmosphere (5% CO_2) at 37 ℃. Commercial PKCβ$_2$ siRNA and Cav-3 siRNA (Santa Cruz Biotechnology) were utilized for inhibition of both PKCβ$_2$ and Cav-3 expression per manufacturer's protocol. After transfection with control, PKCβ$_2$ or Cav-3 siRNA, cells were incubated in either low or high glucose in DMEM medium for 36 hours, and snap frozen in liquid nitrogen.

Determination of myocardial levels of NO, O_2^-, and nitrotyrosine

Frozen heart tissues were pulverized separately with mortar and pestle in liquid nitrogen, homogenized in ice-cold PBS, and centrifuged at 3,000 g for 15 minutes at 4°C for supernatant collection. The supernatant protein concentration was determined via a Lowry assay kit (Bio-Rad, CA, USA). Concentrations of nitrites (NO_2^-) and nitrates (NO_3^-), the stable end products of nitric oxide (NO), were determined by the Griess reaction as previously described(29). NO levels were expressed as nmol/μg protein. Myocardial O_2^- production was determined via lucigeninchemiluminescence method (30, 31). The supernatant samples were loaded with dark-adapted lucigenin (5 μM), and read in 96-well microplates by luminometer (GloMax, Promega), with and without pretreatment with the NOS inhibitor L-NAME (100μM (15)) for 30 minutes at room temperature. Light emission, expressed as mean light units (MLU)/min/100

μg protein, was recorded for 5 minutes. Myocardial nitrotyrosine levels (μg/mg protein) in the collected supernatant were determined by chemiluminescence detection via the Nitrotyrosine Assay Kit per manufacturer's protocol (Millipore, USA).

Separation of cytosol and membrane fractions of heart tissues

In order to characterize subcellular distributions of targeted proteins, cytosol and membrane fractions of cardiac tissue lysate were separated by ultracentrifugation described previously (5). Cytosol and membrane fractions were denatured by 5×SDS loading buffer, and subjected to analysis for PKCβ_1 and PKCβ_2 expression by Western blot as described below.

Isolation of caveolin-rich fractions

Caveolae were isolated by discontinuous sucrose gradient centrifugation as described previously(22). Each heart sample gradient was separated into 12 fractions. Fractions 4-6 were considered the lipid raft fractions, and fractions 8-12 were considered the heavier fractions. Equal protein amounts were loaded for Western blot analysis.

Western blot analysis

Equal protein amounts from isolated cardiomyocytes, H9C2 cells, and rat heart homogenate were resolved by 7.5-12.5% SDS-PAGE and subsequently transferred to PVDF membrane for immunoblot analysis as described previously (32).

Statistical analysis

Densitometry was obtained by image analysis software (Bio-Rad). All values are

presented as means ± S.E.M. Comparisons between multiple groups were made by one-way analysis of variance (ANOVA) followed by Tukey's test for multiple comparisons. Statistical analysis was performed by GraphPad Prism (GraphPad Software Inc., San Diego, CA, USA). P values less than 0.05 were considered significant.

RESULTS

Expression and association of PKCβ$_2$ and Cav-3 in cardiomyocytes isolated from diabetic rats

We previously reported activation of the PKCβ$_2$, but not PKCβ$_1$, isoform in the diabetic heart (6). In the present study, we examined whether PKCβ$_2$ activation was associated with abnormal Cav-3 expression, a muscle-specific marker of caveolae(17). Diabetes moderately increased PKCβ$_2$ phosphorylation on thr-642 residue (data not shown), but the increase in ~~increased~~ phosphorylation of PKCβ$_2$ ~~on~~ was most profound at serine residue 660, without influencing total PKCβ$_2$, resulting in a markedly increased ratio of phosphorylated PKCβ$_2$/total PKCβ$_2$ (Figure 1A ~~and B~~). Decreased Cav-3 expression was observed in cardiomyocytes isolated from 8-week diabetic rat hearts compared to age-matched control (Figure 1B). We next examined the relationship between Cav-3 and PKCβ$_2$ by immunoprecipitation experiments in isolated cardiomyocytes. While a small amount of PKCβ$_2$ remained constitutively associated with Cav-3 during basal conditions, the diabetic condition increased ~~both translocation of PKCβ$_2$, and~~ its association with Cav-3 (Figure 1C). To confirm our findings, we utilized confocal immunofluorescence staining. Limited PKCβ$_2$ was present during basal conditions in association with Cav-3 in the cell

membrane (indicated by scant yellow punctate staining of the cell periphery); 36 hours of high-glucose (HG) stimulation significantly increased regions of co-localization between PKCβ$_2$ and Cav-3 compared to low-glucose (LG) stimulation (Figure 1D).

Effect of high-glucose on expression and association of p-PKCβ$_2$ and Cav-3 in isolated cardiomyocytes over time

High-glucose conditions significantly increased ~~p-PKCβ$_2$ expression~~ the ratio of p-PKCβ$_2$/total PKCβ$_2$ (indicating PKCβ$_2$ activation) in cardiomyocytes within 1 hour, for up to 48 hours (Figure 2A). Peak increase in ~~p-PKCβ$_2$ expression~~ the ratio of p-PKCβ$_2$/total PKCβ$_2$ occurred after 12 hours HG exposure. The osmotic control mannitol exerted no effects upon p-PKCβ$_2$/total PKCβ$_2$ ~~p-PKCβ$_2$~~ and Cav-3 expression (data not shown). In contrast to the quick increase of p-PKCβ$_2$/total PKCβ$_2$ ~~p-PKCβ$_2$ expression~~as early as 1 hour after HG exposure, Cav-3 expression did not significantly increase until 6-12 hours after HG exposure, reduced to basal levels within 24 hours, and significantly decreased 36-48 hours after initial HG exposure (Figure 2B). Cardiomyocyte LDH release significantly increased 24 hours after HG exposure, with rising tendency continuing 36-48 hours after initial HG exposure (Figure 2C).

Hyperglycemia-induced PKCβ$_2$ activation involves caveolae and is associated with reduced Cav-3 expression

We next investigate the interplay between PKCβ$_2$ activation and caveolae (and Cav-3) under hyperglycemic conditions. Given that PKCβ$_1$ activation induced by HG requires caveolae in primary mesangial cells (33), we determined whether caveolae

are crucial in HG-induced PKCβ$_2$ activation in isolated cardiomyocytes from non-diabetic rats. As shown in Figure 3A, phosphorylation of PKCβ$_2$ induced by HG was prevented by either the selective PKCβ$_2$ inhibitor CGP-53353 (CGP, 1μM, from Sigma-Aldrch, USA, IC50 values are 0.41 μM and 3.8 μM respectively for PKCβ$_2$ and PKCβ$_1$) or methyl-β-cyclodextrin (CD, 50 μM, a disrupter of cholesterol-rich caveolae) (34). To determine whether Cav-3 is required for PKCβ$_2$ activation, we subjected H9C2 cells treated with rat-specific Cav3-siRNA to both low- and high-glucose conditions. siRNA-mediated reduction of Cav-3 expression by ~60% (Figure 3B) prevented augmented phosphorylation of PKCβ$_2$ in HG conditions. No effects upon PKCβ$_2$ phosphorylation were observed in cells exposed to ~~normal~~ low glucose (LG) (Figure 3B). We also determined whether excessive PKCβ$_2$ activation induced by HG is associated with reduced Cav-3 expression. Selective inhibition of PKCβ$_2$ activation by CGP reversed the reduction of Cav-3 expression in primary cardiomyocytes exposed to HG (Figure 3C). Similarly, in H9C2 cells, knockdown of PKCβ$_2$ by siRNA reduced PKCβ$_2$ phosphorylation in cells incubated in ~~normal~~ LG and HG conditions (Figure 3D), and attenuated decreased Cav-3 expression in cells exposed to HG, with no impact upon Cav-3 expression in cells exposed to ~~normal glucose~~ LG (Figure 3E).

Hyperglycemia-induced activation of PKCβ$_2$ is associated with caveolae-modulated Akt/eNOS signaling

Next, we investigate the impact of PKCβ$_2$ activation by HG, in the downstream signaling molecules Akt and eNOS, both modulated by caveolins(35). Cardiomyocytes incubated in HG exhibited decreased phosphorylation of Akt at Ser^{473} and eNOS at Ser^{1177}, and these decreases were reversed by CGP treatment

(Figures 4A and B). Caveolar disruption by CD further exaggerated HG-mediated reduction of Akt phosphorylation (Figure 4A), but did not further exacerbate HG-induced reduction of p-eNOS expression (Figure 4B). However, CGP mediated restoration of eNOS phosphorylation in HG-treated cardiomyocytes was abolished during concomitant CD treatment (Figure 4B). To confirm the relative effects of PKCβ_2 and Cav-3 upon HG-mediated changes in p-AKT and p-eNOS, H9C2 cells were subject to both PKCβ_2 and Cav-3 knockdown by siRNA. PKCβ_2 knockdownsignificantly increased the phosphorylation of Akt and eNOS in HG-treated cells, effects which were not observed in LG-treated cells (Figure 4C). Knockdown of Cav-3 resulted in ~~dramatically~~ further reduced expression of both p-Akt and p-eNOS in both LG and HG-treated cells (Figure 4D).

Inhibition of PKCβ_2 activation by ~~specific pharmacologic inhibitor (~~LY333531~~)~~ attenuates cardiac caveolar dysfunction in diabetic rats

To further investigate the role of PKCβ_2 activation in diabetes-induced abnormalities, we treated STZ-induced diabetic rats with the PKCβ inhibitor LY333531 for 4 weeks. PKCβ_2, but not PKCβ_1, ~~–~~isoform was ~~overexpressed~~ excessively activated in the diabetic heart, as demonstrated by increased membrane translocation of PKCβ_2 but not PKCβ_1, a phenomenon inhibited by LY333531 (Figure 5A). PKCβ2-inhibitor LY333531 administration suppressed augmented whole-heart Cav-1 expression (Figure 5B), and prevented whole-heart decreased Cav-3 expression (Figure 5C). Caveolae fractions were isolated via discontinuous sucrose gradient centrifugation of whole cell lysates. Cav-1 was found predominantly in fractions 8-10, whereas Cav-3 was located within both lipid fractions (4-6) and heavier fractions (8-12). PKCβ_2 was predominantly co-expressed within Cav-3-rich fractions (Figure 5D). Densitometric

analysis of all fractions (1-12) demonstrated that PKCβ2-inhibitor LY333531 significantly reduced augmented Cav-1 and $PKC\beta_2$ expression, and suppressed decreased Cav-3 expression in diabetes (Figure 5E).

Inhibition of $PKC\beta_2$ activation by ~~specific pharmacologic inhibitor (~~LY333531~~)~~ attenuates diastolic dysfunction in diabetic rats

At the end of the treatment period, untreated diabetic rats had significantly elevated blood glucose and reduced body weight and heart weight as compared to control rats, which were not altered by LY333531 treatment (Table 1). However, ~~$PKC\beta_2$ inhibitor LY333531 reduced the augmented~~ the ratio of heart-weight to body-weight, an indirect index of myocardial hypertrophy, in the untreated diabetic rats was significantly higher than that in the control rats, which was significantly attenuated by LY333531 treatment (Table 1)~~, while exhibiting no effect upon hyperglycemia degree (Figure 6B)~~. Further, the left ventricular cardiomyocyte cross-sectional areas as assessed in H&E stained cardiac sections (methodology available at Online appendix) in the untreated diabetic rats was significantly bigger than that in the control rats and was significantly attenuated by LY333531 treatment (online appendix Figure 1), showing that LY333531 can attenuate cardiomyocyte hypertrophy in diabetes. We further determined rat cardiac function via echocardiography. As shown in table 1, no significant change in fractional shorting (FS), fractional left ventricular posterior wall thickening (FLVPW), and ejection fraction (EF) was observed among all experimental groups (although non-significant decreased values were recorded in the untreated diabetic group~~, Figure 6C~~). Such data suggests preserved systolic function at ~~4~~ 5 weeks in diabetic rats as used in our model. However, diastolic dysfunction was ~~observed~~ manifested. The~~, as both~~ heart rate (HR) and the ratio of peak velocity of

early and late diastolic filling (E/A) was significantly decreased in diabetic rats as a consequence of significant reduction of E velocity and enhancement of A velocity that was concomitant with significant increase in left ventricular (LV) isovolumic relaxation time (IVRT) and reductions in LV end-diastolic volume (LVVd) and stroke volume (SV). Four weeks treatment with LY333531 restored the values of E/A, IVRT, LVVd and SV to levels that were comparable to that in the control rats but without significant effect upon HR.

~~PKCβ2 inhibitor~~ LY333531 ameliorated diabetic-induced derangements of myocardial NO, O_2^- and nitrotyrosine content, and reverted changes in cardiac Akt, eNOS and iNOS

Diabetes is associated with decreased NO levels, and increased O_2^- and nitrotyrosine production(15, 36), agents of oxidative and nitrative stress. To determine whether ~~PKCβ2 inhibitor~~ LY333531 conferred cardioprotection in part by reducing oxidative and nitrative stress in diabetes, the levels of NO, O_2^-, and nitrotyrosine in diabetic heart tissues were assessed. The diabetic condition significantly decreased NO levels (Figure 6A) and increased O_2^- (Figure 6B) and nitrotyrosine production (Figure 6C) in cardiac tissues. ~~PKCβ2 inhibitor~~ LY333531 suppressed all these derangements. Further studies revealed that the diabetes-induced augmented O_2^- levels could be blocked by the NOS inhibitor L-NAME (100 μM) (Figure 6B), suggesting a NOS-dependent mechanism for O_2^- accumulation. We next investigated related signaling molecules, including Akt, eNOS, and iNOS. The diabetic condition did not affect total cardiac Akt and eNOS expression, but significantly decreased p-Akt (Ser 473) and p-eNOS (Ser 1177) expression, both reversed by LY333531 (Figures 6D and E). Consistent with a recent study (37), our results demonstrated diabetes increased

myocardial iNOS (an adverse marker mediating nitrative stress (24)), which was reversed by LY333531 (Figure 6F).

DISCUSSION

In the present study, we have demonstrated that hyperglycemia-induced cardiac PKCβ$_2$ activation requires caveolae. We provided evidence that excessive PKCβ$_2$ activation is associated with reduced Cav-3 expression, contributing to abnormal Akt/eNOS signaling during hyperglycemia. ~~Selective pharmacologic i~~Inhibition of excessive activation of PKCβ$_2$ by compound LY333531 improves cardiac diastolic function, possibly via attenuation of caveolar dysfunction and rescuing Akt/eNOS/NO function in the diabetic heart. To our best knowledge, this is the first study examining the relationship between PKCβ$_2$ and Cav-3 in cardiomyocytes subjected to hyperglycemic conditions.

It is well-established that chronic hyperglycemia induces abnormal activation of PKC, which contributes to diabetic cardiovascular complications(38, 39). However, the PKC signaling pathway is complicated by numerous isoforms, each with varying cellular distribution and opposing function at times (40). The PKCβ$_2$ isoform is most frequently implicated in diabetic cardiovascular complications (5-8). Our current study further confirmed that PKCβ$_2$, but not PKCβ$_1$, is excessively activated in the diabetic heart. Although the precise mechanisms by which hyperglycemia induces PKCβ$_2$ activation in cardiomyocytes are not fully understood, evidence supports the vital role of caveolae (the specialized plasma membrane microdomains modulating signaling transduction pathways of molecules docked within them (17)) in hyperglycemia-induced PKCβ$_2$ activation. This is well supported by our immunoprecipitation and immunofluorescence studies demonstrating hyperglycemia increased the association and co-localization of PKCβ$_2$ and Cav-3. Caveolar disruption by methyl-β-cyclodextrin(34) suppressed hyperglycemia-induced PKCβ$_2$ activation in isolated cardiomyocytes. Cav-3 knockdown by siRNA prevented

augmented PKCβ$_2$ phosphorylation in H9C2 cells exposed to high-glucose, suggesting that Cav-3 is required specifically for hyperglycemia-induced PKCβ$_2$ activation in cardiomyocytes.

Cav-3 is the predominant cardiomyocyte caveolin isoform essential for caveolar function. In the current study, we demonstrated that cardiomyocyte Cav-3 expression increased 6-12 hours after HG exposure but reduced to basal levels within 24 hours and progressively further reduced to lower than basal levels after 36 to 48 hours of HG exposure. The initial increase in Cav-3 expression after HG exposure observed in our study is an acute response to the calorie surplus similar to that reported by other researchers(41). The significant reduction of Cav-3 expression in cardiomyocytes after prolonged HG exposure is consistent with our results from the intact rats which showed that Cav-3 expression was decreased in isolated cardiomyocytes from rats of 8- and ~~4~~5-week duration of diabetic condition. Loss of Cav-3 expression results in cardiomyopathy(42), and reduction in cardiac Cav3 protein expression is highly correlated with reduction in ~~and is associated with~~ left ventricular fractional shortening ~~dysfunction~~ in mice with constitutive overexpression of A1-adenosine receptor induced cardiac dilatation and dysfunction, and with makers of heart failure phenotype in humans ~~in murine heart failure models and in human heart failure~~ (43). Our study results suggest excess PKCβ$_2$ activation contributes towards attenuated Cav-3 expression in the diabetic heart, as inhibition of PKCβ$_2$ activation by CGP53353 or siRNA-mediated PKCβ$_2$ expression knockdown prevented the decline of Cav-3 expression in cells exposed to HG. ~~Additionally, pharmacologic inhibition of PKCβ$_2$ by~~ LY333531 treatment ameliorated diabetic heart ~~caveolar~~ caveolae dysfunction.

PKCβ$_2$ activation likely exerts adverse effects in the diabetic heart via alteration of the

Akt/eNOS signaling pathway, which is modulated by caveolins(35). Although Cav-1 negatively regulates eNOS in cardiovascular tissues (44, 45), the co-localization of Cav-3 and eNOS may facilitate eNOS activation by both cell surface receptors and cellular surface NO release for intercellular signaling in cardiomyocytes(18). This is supported by our findings that disruption of caveolae function by methyl-β-cyclodextrin or Cav-3 siRNA prevented Akt phosphorylation and suppressed eNOS phosphorylation in cardiomyocytes. Additionally, hyperglycemia decreased phosphorylated Akt and eNOS in both isolated cardiomyocytes and in diabetic heart tissues, leading to decreased myocardial NO levels, reduced Cav-3 levels, and increased Cav-1 cardiac levels. Inhibition of PKCβ_2 activation suppressed or abrogated these alterations. Therefore, inhibition of PKCβ_2 activation may rescue proper Akt/eNOS/NO signaling in the diabetic heart via caveolin regulation.

Previous studies have demonstrated involvement of increased iNOS expression with cardiovascular abnormalities in STZ-induced diabetic rats (24, 46). Our study confirms increased iNOS cardiac content in diabetic rats, an adverse mediator of nitrative stress (24), and increased nitrotyrosine was also demonstrated in diabetic heart tissue. The NOS inhibitor L-NAME blocked diabetes-induced augmentation of O_2^- levels, indicating eNOS uncoupling, which is in line with a recent study in STZ-induced diabetic mice (47). Furthermore, treatment of diabetic rats with ~~PKCβ_2 inhibitor~~ LY333531 inhibited cardiac iNOS expression and reduced both nitrotyrosine and O_2^- production. Diabetes is associated with decreased NO levels and increased O_2^- and nitrotyrosine production (15, 36), which are implicated with oxidative/nitrative stress and eNOS uncoupling. Our study provides direct evidence showing that inhibition of PKCβ_2 activation can mitigate oxidative/nitrative stress and eNOS uncoupling.

Initial left ventricular diastolic dysfunction, reduced contractility, and prolonged diastole are the hallmarks of diabetic cardiomyopathy (48, 49). In the present study, ~~echocardiography revealed that diabetes decreased the ratio of peak velocity of early and late diastolic filling (E/A)~~ diabetes significantly reduced E/A ratio that was concomitant with significantly increased ~~left ventricular isovolumic relaxation time (~~IVRT and decreased LVVd and SV, but did not alter fractional shorting (FS), fractional left ventricular posterior wall thickening (FLVPW) or ejection fraction (EF). Such data indicates that myocardial diastolic (but not systolic) dysfunction occurs in 4~~5~~-week STZ-induced diabetic rats, which can be ameliorated by ~~PKCβ2 inhibition with~~ LY333531. ~~-mediated PKCβ$_2$ inhibition a potentially efficacious approach for preserving cardiac function in diabetic cardiomyopathy~~. Our findings are in general agreement with the findings of Mihm MJ et al (27) who conducted a series study in a similar STZ-diabetic rats and showed that diastolic dysfunction occurred early during the course of the disease which progressed to LV dilation reflected as increases in LVIDd and LVIDs with concomitant increase in LV luminal area and systolic dysfunction reflected as reduction in LV FS 35 days after STZ-injection and onward. It should be noted that the E/A ratio derived from the conventional Doppler echocardiography as used in our current study is not a load-independent parameter and may have inherent limitations, such as the peak E wave velocity can be highly dependent upon heart rate(27), while the heart rate in the diabetic rats was lower than that in the control group (Table 1). The newly developed Doppler tissue echocardiography (DTE) can acquire myocardial wall and mitral annular velocity online and the early diastolic annular velocity measured using DTE has been reported to be a preload independent index for evaluating LV diastolic function. A combination of DTE derived E'/A' ratio and the mitral inflow patterns (E/A ratio) obtained by

conventional Doppler echocardiography in future studies should help to provide better estimations of diastolic dysfunction. However, the significant reduction of E/A ratio as a consequence of significant reduction of E velocity and significant enhancement of A velocity in combination with concomitant increase in IVRT and reductions in LVVD and SV in the diabetic group could jointly suggest diastolic dysfunction in the current study. LY333531 treatment in diabetic rats did not affect heart rate but corrected all the above changes, suggesting the LY333531 treatment prevented the development of diastolic dysfunction. Future functional study with cardiomyocytes isolated from various stages of diabetes rodents will help establish the relative contribution of the slowing in cardiomyocyte relaxation time and left ventricular stiffness (due to fibrosis) to the development of diastolic dysfunction.

In summary, our study demonstrates that hyperglycemia-induced PKCβ_2 activation is associated with caveolar dysfunction, and consequently deranged Akt/eNOS signaling (Figure ~~8~~ 7). Inhibition of PKCβ_2 activation attenuated cardiac diastolic dysfunction by restoring caveolin-3 expression and subsequently rescuing Akt/eNOS/NO signaling. PKCβ_2 blockade may therefore represent a novel therapeutic avenue in the treatment of diabetic cardiomyopathy.

ACKNOWLEDGMENTS

This study was supported by a grant from the National Natural Science Foundation of China (NSFC 81270899), and in part by a General Research Fund grant (784011M and 782910M) from the Research Grants Council of Hong Kong.

S.L. performed the study and wrote the manuscript. H.L., J.X., Y.L. and X.G. performed the study. J.W., K.N., W.L., X.M., B.R. contributed to data analysis and interpretation. M.I and Z.X reviewed/approved the research protocol. Z. X wrote the manuscript. Z. X takes full responsibility for the work as a whole, including the study design, access to data, and the decision to submit and publish the manuscript.

REFERENCES

1. Khavandi K, Khavandi A, Asghar O, Greenstein A, Withers S, Heagerty AM, Malik RA: Diabetic cardiomyopathy--a distinct disease? *Best Pract Res Clin Endocrinol Metab* 23: 347-360, 2009
2. Zarich SW,Nesto RW: Diabetic cardiomyopathy. *American heart journal* 118: 1000-1012, 1989
3. Kim DH, Kim YJ, Chang SA, Lee HW, Kim HN, Kim HK, Chang HJ, Sohn DW, Park YB: The protective effect of thalidomide on left ventricular function in a rat model of diabetic cardiomyopathy. *European journal of heart failure* 12: 1051-1060, 2010
4. Ni Q, Wang J, Li EQ, Zhao AB, Yu B, Wang M, Huang CR: Study on the protective effect of shengmai san (see text) on the myocardium in the type 2 diabetic cardiomyopathy model rat. *Journal of traditional Chinese medicine = Chung i tsa chih ying wen pan / sponsored by All-China Association of Traditional Chinese Medicine, Academy of Traditional Chinese Medicine* 31: 209-219, 2011
5. Xia Z, Kuo KH, Nagareddy PR, Wang F, Guo Z, Guo T, Jiang J, McNeill JH: N-acetylcysteine attenuates PKCbeta2 overexpression and myocardial hypertrophy in streptozotocin-induced diabetic rats. *Cardiovasc Res* 73: 770-782, 2007
6. Liu Y, Lei S, Gao X, Mao X, Wang T, Wong GT, Vanhoutte PM, Irwin MG, Xia Z: PKCbeta inhibition with ruboxistaurin reduces oxidative stress and attenuates left ventricular hypertrophy and dysfuntion in rats with streptozotocin-induced diabetes. *Clin Sci (Lond)* 122: 161-173, 2012
7. Gurusamy N, Watanabe K, Ma M, Zhang S, Muslin AJ, Kodama M, Aizawa Y: Inactivation of 14-3-3 protein exacerbates cardiac hypertrophy and fibrosis through enhanced expression of protein kinase C beta 2 in experimental diabetes. *Biol Pharm Bull* 28: 957-962, 2005
8. Way KJ, Isshiki K, Suzuma K, Yokota T, Zvagelsky D, Schoen FJ, Sandusky GE, Pechous PA, Vlahos CJ, Wakasaki H, King GL: Expression of connective tissue growth factor is increased in injured myocardium associated with protein kinase C beta2 activation and diabetes. *Diabetes* 51: 2709-2718, 2002
9. Wei L, Yin Z, Yuan Y, Hwang A, Lee A, Sun D, Li F, Di C, Zhang R, Cao F, Wang H: A PKC-beta inhibitor treatment reverses cardiac microvascular barrier dysfunction in diabetic rats. *Microvasc Res* 80: 158-165, 2010
10. Connelly KA, Kelly DJ, Zhang Y, Prior DL, Advani A, Cox AJ, Thai K, Krum H, Gilbert RE: Inhibition of protein kinase C-beta by ruboxistaurin preserves cardiac function and reduces extracellular matrix production in diabetic cardiomyopathy. *Circ Heart Fail* 2: 129-137, 2009
11. Clarke M,Dodson PM: PKC inhibition and diabetic microvascular complications. *Best practice & research. Clinical endocrinology &*

metabolism 21: 573-586, 2007

12. Simpson PC: Beta-protein kinase C and hypertrophic signaling in human heart failure. *Circulation* 99: 334-337, 1999
13. Connelly KA, Kelly DJ, Zhang Y, Prior DL, Advani A, Cox AJ, Thai K, Krum H, Gilbert RE: Inhibition of protein kinase C-beta by ruboxistaurin preserves cardiac function and reduces extracellular matrix production in diabetic cardiomyopathy. *Circulation. Heart failure* 2: 129-137, 2009
14. Naruse K, Rask-Madsen C, Takahara N, Ha SW, Suzuma K, Way KJ, Jacobs JR, Clermont AC, Ueki K, Ohshiro Y, Zhang J, Goldfine AB, King GL: Activation of vascular protein kinase C-beta inhibits Akt-dependent endothelial nitric oxide synthase function in obesity-associated insulin resistance. *Diabetes* 55: 691-698, 2006
15. Ren J, Duan J, Thomas DP, Yang X, Sreejayan N, Sowers JR, Leri A, Kajstura J, Gao F, Anversa P: IGF-I alleviates diabetes-induced RhoA activation, eNOS uncoupling, and myocardial dysfunction. *Am J Physiol Regul Integr Comp Physiol* 294: R793-802, 2008
16. Rybin VO, Xu X, Steinberg SF: Activated protein kinase C isoforms target to cardiomyocyte caveolae : stimulation of local protein phosphorylation. *Circ Res* 84: 980-988, 1999
17. Panneerselvam M, Patel HH, Roth DM: Caveolins and heart diseases. *Adv Exp Med Biol* 729: 145-156, 2012
18. Feron O,Balligand JL: Caveolins and the regulation of endothelial nitric oxide synthase in the heart. *Cardiovasc Res* 69: 788-797, 2006
19. Kempf T,Wollert KC: Nitric oxide and the enigma of cardiac hypertrophy. *Bioessays* 26: 608-615, 2004
20. Fujita T, Otsu K, Oshikawa J, Hori H, Kitamura H, Ito T, Umemura S, Minamisawa S, Ishikawa Y: Caveolin-3 inhibits growth signal in cardiac myoblasts in a Ca2+-dependent manner. *J Cell Mol Med* 10: 216-224, 2006
21. Penumathsa SV, Thirunavukkarasu M, Zhan L, Maulik G, Menon VP, Bagchi D, Maulik N: Resveratrol enhances GLUT-4 translocation to the caveolar lipid raft fractions through AMPK/Akt/eNOS signalling pathway in diabetic myocardium. *J Cell Mol Med* 12: 2350-2361, 2008
22. Penumathsa SV, Thirunavukkarasu M, Samuel SM, Zhan L, Maulik G, Bagchi M, Bagchi D, Maulik N: Niacin bound chromium treatment induces myocardial Glut-4 translocation and caveolar interaction via Akt, AMPK and eNOS phosphorylation in streptozotocin induced diabetic rats after ischemia-reperfusion injury. *Biochim Biophys Acta* 1792: 39-48, 2009
23. Galvez MI: Protein kinase C inhibitors in the treatment of diabetic retinopathy. Review. *Curr Pharm Biotechnol* 12: 386-391, 2011
24. Nagareddy PR, Soliman H, Lin G, Rajput PS, Kumar U, McNeill JH, MacLeod KM: Selective inhibition of protein kinase C beta(2) attenuates inducible nitric oxide synthase-mediated cardiovascular abnormalities in

streptozotocin-induced diabetic rats. *Diabetes* 58: 2355-2364, 2009

25. Ishii H, Jirousek MR, Koya D, Takagi C, Xia P, Clermont A, Bursell SE, Kern TS, Ballas LM, Heath WF, Stramm LE, Feener EP, King GL: Amelioration of vascular dysfunctions in diabetic rats by an oral PKC beta inhibitor. *Science* 272: 728-731, 1996
26. Gao X, Xu Y, Xu B, Liu Y, Cai J, Liu HM, Lei S, Zhong YQ, Irwin MG, Xia Z: Allopurinol attenuates left ventricular dysfunction in rats with early stage of streptozotocin-induced diabetes. *Diabetes Metab Res Rev*, 2012
27. Mihm MJ, Seifert JL, Coyle CM, Bauer JA: Diabetes related cardiomyopathy time dependent echocardiographic evaluation in an experimental rat model. *Life Sci* 69: 527-542, 2001
28. Wang T, Qiao S, Lei S, Liu Y, Ng KF, Xu A, Lam KS, Irwin MG, Xia Z: N-acetylcysteine and allopurinol synergistically enhance cardiac adiponectin content and reduce myocardial reperfusion injury in diabetic rats. *PLoS One* 6: e23967, 2011
29. Luo T, Xia Z, Ansley DM, Ouyang J, Granville DJ, Li Y, Xia ZY, Zhou QS, Liu XY: Propofol dose-dependently reduces tumor necrosis factor-alpha-Induced human umbilical vein endothelial cell apoptosis: effects on Bcl-2 and Bax expression and nitric oxide generation. *Anesth Analg* 100: 1653-1659, 2005
30. Li YL, Gao L, Zucker IH, Schultz HD: NADPH oxidase-derived superoxide anion mediates angiotensin II-enhanced carotid body chemoreceptor sensitivity in heart failure rabbits. *Cardiovasc Res* 75: 546-554, 2007
31. Li JM,Shah AM: Mechanism of endothelial cell NADPH oxidase activation by angiotensin II. Role of the p47phox subunit. *J Biol Chem* 278: 12094-12100, 2003
32. Lei S, Liu Y, Liu H, Yu H, Wang H, Xia Z: Effects of N-acetylcysteine on nicotinamide dinucleotide phosphate oxidase activation and antioxidant status in heart, lung, liver and kidney in streptozotocin-induced diabetic rats. *Yonsei Med J* 53: 294-303, 2012
33. Zhang Y, Peng F, Gao B, Ingram AJ, Krepinsky JC: High glucose-induced RhoA activation requires caveolae and PKCbeta1-mediated ROS generation. *Am J Physiol Renal Physiol* 302: F159-172, 2012
34. Christian AE, Haynes MP, Phillips MC, Rothblat GH: Use of cyclodextrins for manipulating cellular cholesterol content. *J Lipid Res* 38: 2264-2272, 1997
35. Krajewska WM,Maslowska I: Caveolins: structure and function in signal transduction. *Cell Mol Biol Lett* 9: 195-220, 2004
36. Jin HR, Kim WJ, Song JS, Piao S, Choi MJ, Tumurbaatar M, Shin SH, Yin GN, Koh GY, Ryu JK, Suh JK: Intracavernous delivery of a designed angiopoietin-1 variant rescues erectile function by enhancing endothelial regeneration in the streptozotocin-induced diabetic mouse. *Diabetes* 60:

969-980, 2011
37. Cheng YS, Dai DZ, Ji H, Zhang Q, Dai Y: Sildenafil and FDP-Sr attenuate diabetic cardiomyopathy by suppressing abnormal expression of myocardial CASQ2, FKBP12.6, and SERCA2a in rats. *Acta Pharmacol Sin* 32: 441-448, 2011
38. Geraldes P,King GL: Activation of protein kinase C isoforms and its impact on diabetic complications. *Circ Res* 106: 1319-1331, 2010
39. Danis RP,Sheetz MJ: Ruboxistaurin: PKC-beta inhibition for complications of diabetes. *Expert Opin Pharmacother* 10: 2913-2925, 2009
40. Mellor H,Parker PJ: The extended protein kinase C superfamily. *Biochem J* 332 (Pt 2): 281-292, 1998
41. Gomez-Ruiz A, de Miguel C, Campion J, Martinez JA, Milagro FI: Time-dependent regulation of muscle caveolin activation and insulin signalling in response to high-fat diet. *FEBS letters* 583: 3259-3264, 2009
42. Woodman SE, Park DS, Cohen AW, Cheung MW, Chandra M, Shirani J, Tang B, Jelicks LA, Kitsis RN, Christ GJ, Factor SM, Tanowitz HB, Lisanti MP: Caveolin-3 knock-out mice develop a progressive cardiomyopathy and show hyperactivation of the p42/44 MAPK cascade. *J Biol Chem* 277: 38988-38997, 2002
43. Feiner EC, Chung P, Jasmin JF, Zhang J, Whitaker-Menezes D, Myers V, Song J, Feldman EW, Funakoshi H, Degeorge BR, Jr., Yelamarty RV, Koch WJ, Lisanti MP, McTiernan CF, Cheung JY, Bristow MR, Chan TO, Feldman AM: Left ventricular dysfunction in murine models of heart failure and in failing human heart is associated with a selective decrease in the expression of caveolin-3. *J Card Fail* 17: 253-263, 2011
44. Elcioglu KH, Kabasakal L, Cetinel S, Conturk G, Sezen SF, Ayanoglu-Dulger G: Changes in caveolin-1 expression and vasoreactivity in the aorta and corpus cavernosum of fructose and streptozotocin-induced diabetic rats. *Eur J Pharmacol* 642: 113-120, 2010
45. Lam TY, Seto SW, Lau YM, Au LS, Kwan YW, Ngai SM, Tsui KW: Impairment of the vascular relaxation and differential expression of caveolin-1 of the aorta of diabetic +db/+db mice. *Eur J Pharmacol* 546: 134-141, 2006
46. Nagareddy PR, Xia Z, McNeill JH, MacLeod KM: Increased expression of iNOS is associated with endothelial dysfunction and impaired pressor responsiveness in streptozotocin-induced diabetes. *Am J Physiol Heart Circ Physiol* 289: H2144-2152, 2005
47. Roe ND, Thomas DP, Ren J: Inhibition of NADPH oxidase alleviates experimental diabetes-induced myocardial contractile dysfunction. *Diabetes Obes Metab* 13: 465-473, 2011
48. Norby FL, Aberle NS, 2nd, Kajstura J, Anversa P, Ren J: Transgenic overexpression of insulin-like growth factor I prevents streptozotocin-induced cardiac contractile dysfunction and beta-adrenergic response in

ventricular myocytes. *J Endocrinol* 180: 175-182, 2004

49. Palmieri V, Capaldo B, Russo C, Iaccarino M, Pezzullo S, Quintavalle G, Di Minno G, Riccardi G, Celentano A: Uncomplicated type 1 diabetes and preclinical left ventricular myocardial dysfunction: insights from echocardiography and exercise cardiac performance evaluation. *Diabetes Res Clin Pract* 79: 262-268, 2008

Table 1

General characteristics and echocardiographic assessment of left ventricle dimensions and functions in rats

	C	D	D+LY
Blood glucose (mM)	6.26±0.53	28.24±4.64**	27.32±3.43**
Body weight (g)	490.1±14.3	295.4±28.8*	371.1±17.4*
Heart weight (g)	1.66±0.15	1.25±0.18*	1.31±0.16*
Heart weight/bodyweight (mg/g)	3.39±0.07	4.23±0.06*	3.53±0.08#
HR (bpm)	332±7.8	270±10.8*	286±9.2*
LVIDs (mm)	4.75±0.43	4.68±0.41	4.74±0.49
LVIDd (mm)	8.29±0.53	7.61±0.62	8.13±0.49
FS (%)	42.70±4.13	38.50±5.42	41.53±3.84
IVSs (mm)	2.23±0.16	2.28±0.07	2.27±0.13
IVSd (mm)	1.72±0.05	1.75±0.05	1.73±0.06
LVPWs (mm)	2.90±0.08	2.92±0.07	2.91±0.06
LVPWd (mm)	1.85±0.06	1.91±0.09	1.87±0.08
LVPW (%)	56.76±7.50	52.88±10.03	55.61±4.81
LVVs (μL)	107.6±15.8	109.8±13.7	114.5±11.9
LVVd (μL)	378.7±25.6	315.4±21.8*	380.4±19.7#
EF (%)	71.6±4.7	65.2±5.7	69.9±3.9
IVRT (ms)	21.75±1.25	27.83±1.80*	20.63±1.38#
E Velocity (cm/s)	1340.9±44.6	1217.8±33.7*	1331.0±40.8#
A Velocity (cm/s)	890.1±37.1	1023.4±34.7*	917.9±28.9#

E/A	1.49±0.09	1.19±0.05*	1.45±0.085#
SV (μL)	285.7±19.1	230.8±17.9*	279.4±20.8#

Control or STZ-induced diabetic rats were either untreated or treated with PKCβ inhibitor LY333531 (LY, 1 mg/kg/day) by oral gavage for four weeks. HR, heart rate; LV, left ventricle; LVIDs, LV internal systolic diameter; LVIDd, LV internal diastolic diameter; FS, fractional shortening; IVSs, systolic interventricular septal thickness; IVSd, diastolic interventricular septal thickness; LVPWs, LV systolic posterior wall thickness; LVPWd, LV diastolic posterior wall thickness; LVVs, LV end-systolic volume; LVVd, LV end-diastolic volume; EF, ejection fraction; IVRT, isovolumetric relaxation time; SV, stroke volume. All the results are expressed as means ± S.E.M., n = 8, control (C), diabetes (D), LY333531 (LY). $^{*}P < 0.05$, $^{**}P < 0.01$ vs. C; $^{\#}P < 0.05$ vs. D.

Titles and legends to figures

Figure 1. Expression of PKCβ$_2$ and Cav-3 in cardiomyocytes isolated from control and STZ-induced diabetic rats (8-weeks). (A) Representative Western blot demonstrating p-PKCβ$_2$ (Ser 660) and total-PKCβ$_2$ expression. (B) Representative Western blot demonstrating Cav-3 expression with GAPDH as loading control. (C) Cell lysates containing equal amounts of total protein were subjected to immunoprecipitation with anti-Cav-3 antibody, and analyzed by immunoblot with PKCβ$_2$ and Cav-3 antibody. All results expressed as means ± S.E.M., n=6-8 per group, $^{*}P<0.05$ vs. control. (D) Confocal laser microscopic image of adult rat cardiomyocytes in response to high glucose. Isolated cardiomyocytes from non-diabetic rats were incubated with low or high glucose for 36 hours, and underwent standard immunofluorescent staining with PKCβ$_2$ and Cav-3 antibodies (see Methods).

Figure 2. Effects of high glucose upon p-PKCβ$_2$ (Ser-660) and Cav-3 expression and LDH release in cultured cardiomyocytes over time. Representative Western blot of p-PKCβ$_2$ (Ser 660) expression in comparison with (A) total-PKCβ$_2$ and (B) Cav-3 expression with GAPDH as loading control. (C) Effects of high glucose upon LDH release. $^{*}P<0.05$ vs. control (time "0") group.

Figure 3. Expression of p-PKCβ$_2$ and Cav-3 in cultured cardiomyocytes and H9C2 cells following various treatments in low (5.5 mM) or high (25 mM) glucose conditions for 36 hours. (A) Representative Western blot demonstrating p-PKCβ$_2$ (Ser

660) in comparison to total-PKCβ$_2$ in cardiomyocytes exposed to high glucose in the presence of a selective PKCβ$_2$ inhibitor CGP-53353 (CGP, 1μM) or methyl-β-cyclodextrin (CD, 10 μM). (B) Representative Western blot demonstrating p-PKCβ$_2$ and Cav-3 expression in H9C2 cells transfected with Cav-3 siRNA, exposed to low or high glucose. (C) Representative Western blot demonstrating Cav-3 expression in cultured cardiomyocytes exposed to high glucose in the presence of CGP (1μM). Representative Western blot demonstrating (D) p-PKCβ$_2$, total PKCβ$_2$ expression, and (D) Cav-3 expression in H9C2 cells transfected with PKCβ$_2$siRNA in low or high glucose conditions. GADPH served as loading control. All results are expressed as means ± S.E.M., n=7, $^{*}P<0.05$ vs. all other groups, $^{\#}P<0.05$ vs. control-siRNA treated groups.

Figure 4. Expression of p-Akt (Ser 473) and p-eNOS (Ser 1177) in cultured cardiomyocytes and H9C2 cells in various treatments in low (5.5 mM) or high glucose (25 mM) conditions for 36 hours. (A) Representative Western blot demonstrating p-Akt in comparison to total Akt, and (B) p-eNOS in comparison with total eNOS in cardiomyocytes exposed to high glucose in the presence of a selective PKCβ$_2$ inhibitor CGP-53353 (CGP, 1μM), methyl-β-cyclodextrin (CD, 10 μM), or CGP+CD combination. Representative Western blot demonstrating p-Akt and p-eNOS expression in H9C2 cells transfected with (C) PKCβ$_2$siRNA or (D) Cav-3 siRNA in low or high glucose conditions. GAPDH served as loading control. All results are expressed as means ± S.E.M., n=7, $^{*}P<0.05$ vs. all other groups, $^{\#}P<0.05$ vs. control-siRNA treated groups.

Figure 5. Effects of PKCβ inhibitor (LY333531) treatment upon subcellular

distributions of PKCβ_1 and PKCβ_2, and expression levels of Cav-1 and Cav-3 in total heart preparations and various isolated cellular fractions. Control (C) or STZ-induced diabetic rats were treated with PKCβ inhibitor LY333531 (1 mg/kg/day, D+LY) or control (D) by oral gavage for four weeks. (A) Representative Western blot demonstrating PKCβ_1 and PKCβ_2 protein expression. GAPDH and Na-K-ATPase served as loading controls in cytosol fractions or membrane fractions respectively. (Bottom graph) Membrane:cytosol ratio as indexes of PKCβ isoform translocation. Representative Western blot demonstrating (B) Cav-1 and (C) Cav-3 content in total heart preparations. (D) Sucrose gradient centrifugation isolated caveolae-enriched fractions. Aliquots containing equal amounts of protein or a volume equal to that of the fraction with the least detectable amount of protein for "protein-free" fractions (1 and 2), and unfractionated samples (UF) were probed for Cav-1, Cav-3, and PKC$\beta_2$immunoreactivity. (E) Cav-1 and Cav-3 and PKCβ_2 expression in all the fractions (1-12) were calculated by relative densitometric values, and expressed as percentage of control. All results expressed as means ± S.E.M., n=7, $^{*}P<0.05$ vs. all other groups.

~~**Figure 6.**Effects of PKCβ inhibitor (LY333531) treatment upon general characteristics and cardiac function of diabetic rats. Control (C) or STZ-induced diabetic rats were treated with PKCβ inhibitor LY333531 (1 mg/kg/day, D+LY) or control (D) by oral gavage for four weeks. Effects of LY333531 upon the (A) ratio of heart weight to body weight and (B) plasma glucose. (C) Effects of LY333531 upon heart rate (HR), fractional shortening (FS), fractional left ventricular posterior wall thickening (FLVPW), ejection fraction (EF), left ventricular isovolumic relaxation time (IVRT), and the ratio of peak velocity of early and late diastolic filling (E/A). All~~

~~results expressed as means ± S.E.M., n=7, *P<0.05 vs. all other groups.~~

Figure ~~7~~ 6. Effects of PKCβ inhibitor (LY333531) treatment upon the levels of NO, O_2^-, nitrotyrosine, and protein expression of p-Akt, p-eNOS, and iNOS in diabetic myocardium. Control (C) or STZ-induced diabetic rats were treated with PKCβ inhibitor LY333531 (1 mg/kg/day, D+LY) or control (D) by oral gavage for four weeks. Effects of LY333531 upon (A) myocardial NO levels, (B) O_2^- levels in the absence and presence of L-NAME, and (C) nitrotyrosine levels; Representative Western blot of (D) p-Akt compared to total Akt, (E) p-eNOS compared to total eNOS, and (F) iNOS with GAPDH as loading control. All results expressed as means ± S.E.M., n=7, *P<0.05 vs. all other groups.

Figure ~~8~~ 7. Schematic depicting hyperglycemia-induced PKCβ2 activation effects upon Cav-3-modulated Akt/eNOS signaling pathway.Cardiomyocytecaveolae are required for hyperglycemia-induced $PKC\beta_2$ activation (translocation from cytosol to caveolae membrane). Excessive $PKC\beta_2$activation decreased cav-3 expression, impairing the Akt/eNOS signaling pathway. Solid arrows depict stimulation, while transverse "T" shape indicates inhibition.

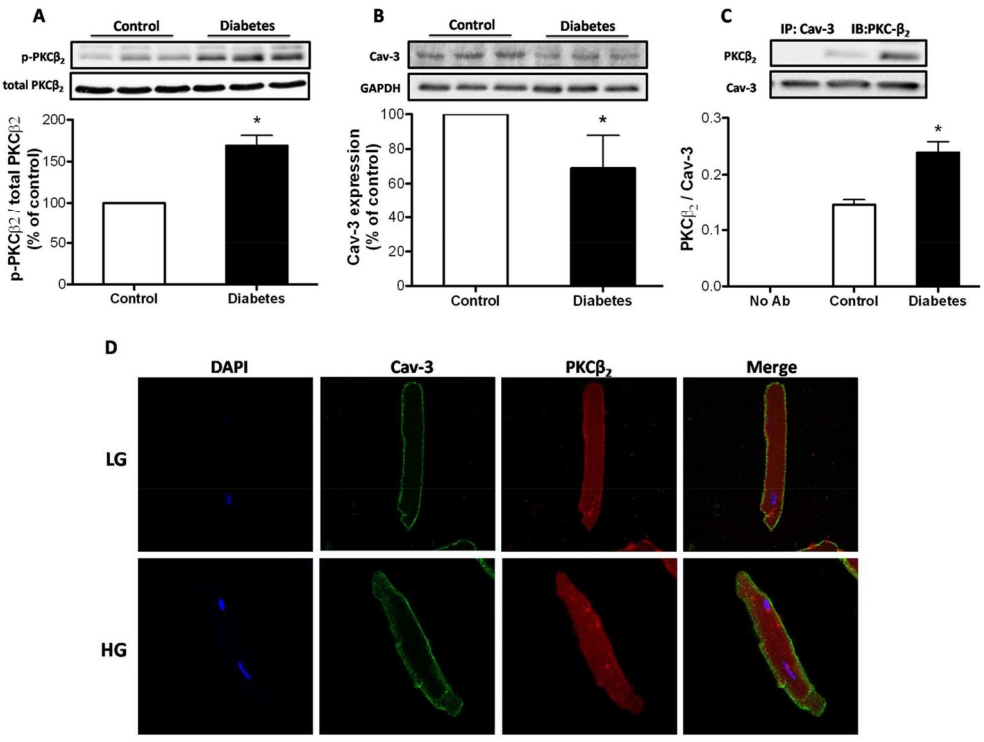

Fig-1
134x101mm (300 x 300 DPI)

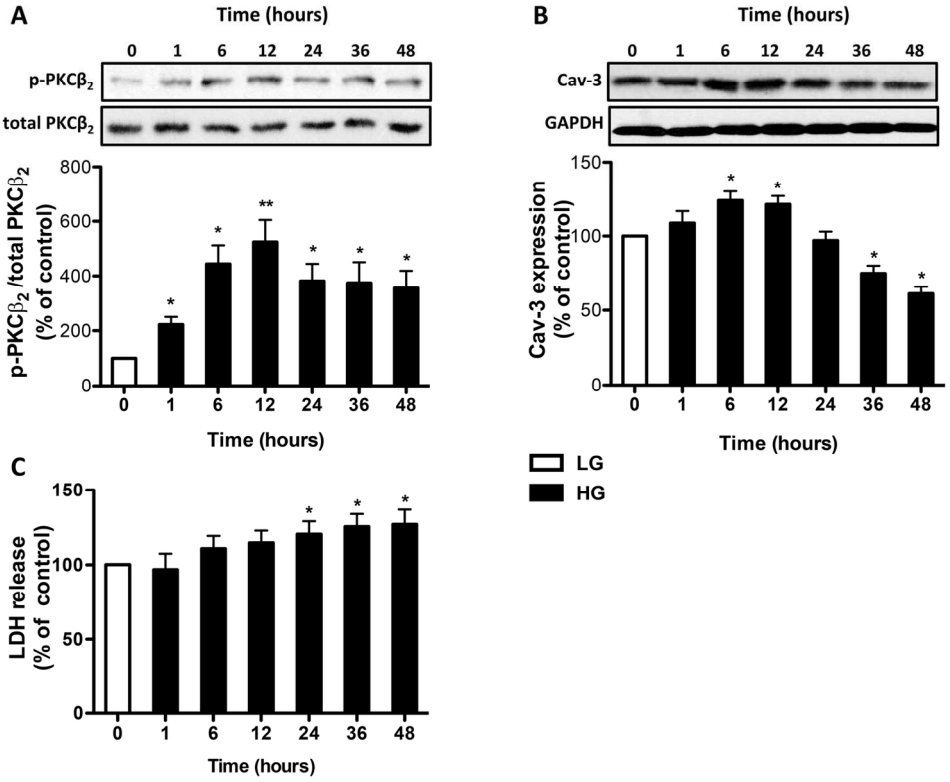

Fig-2
147x120mm (300 x 300 DPI)

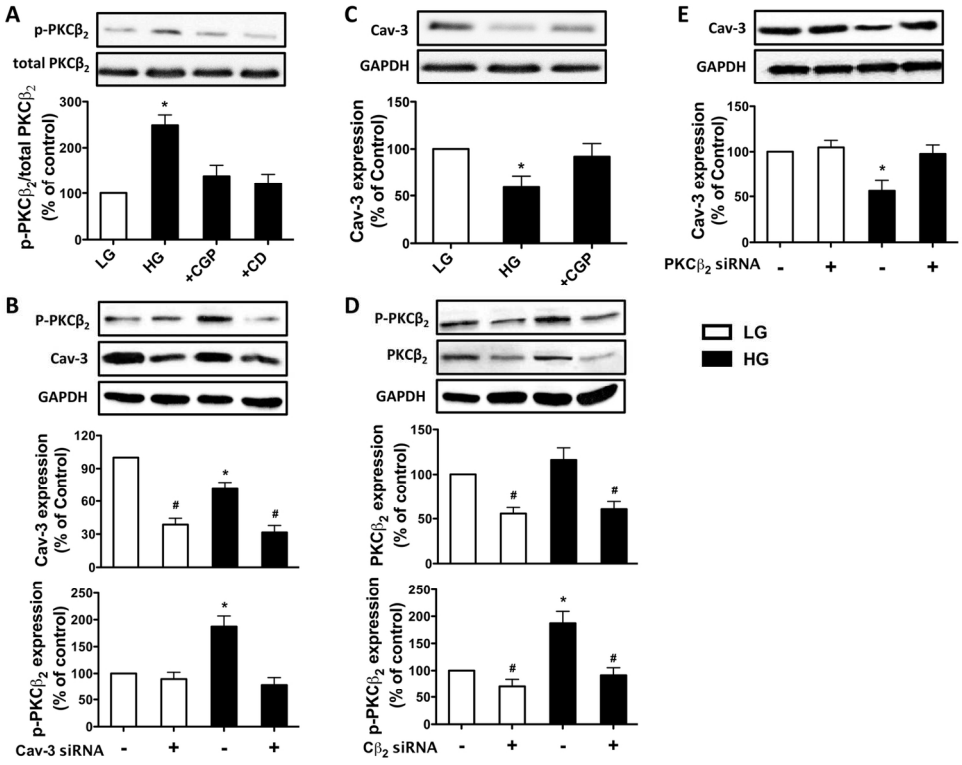

Fig-3
145x117mm (300 x 300 DPI)

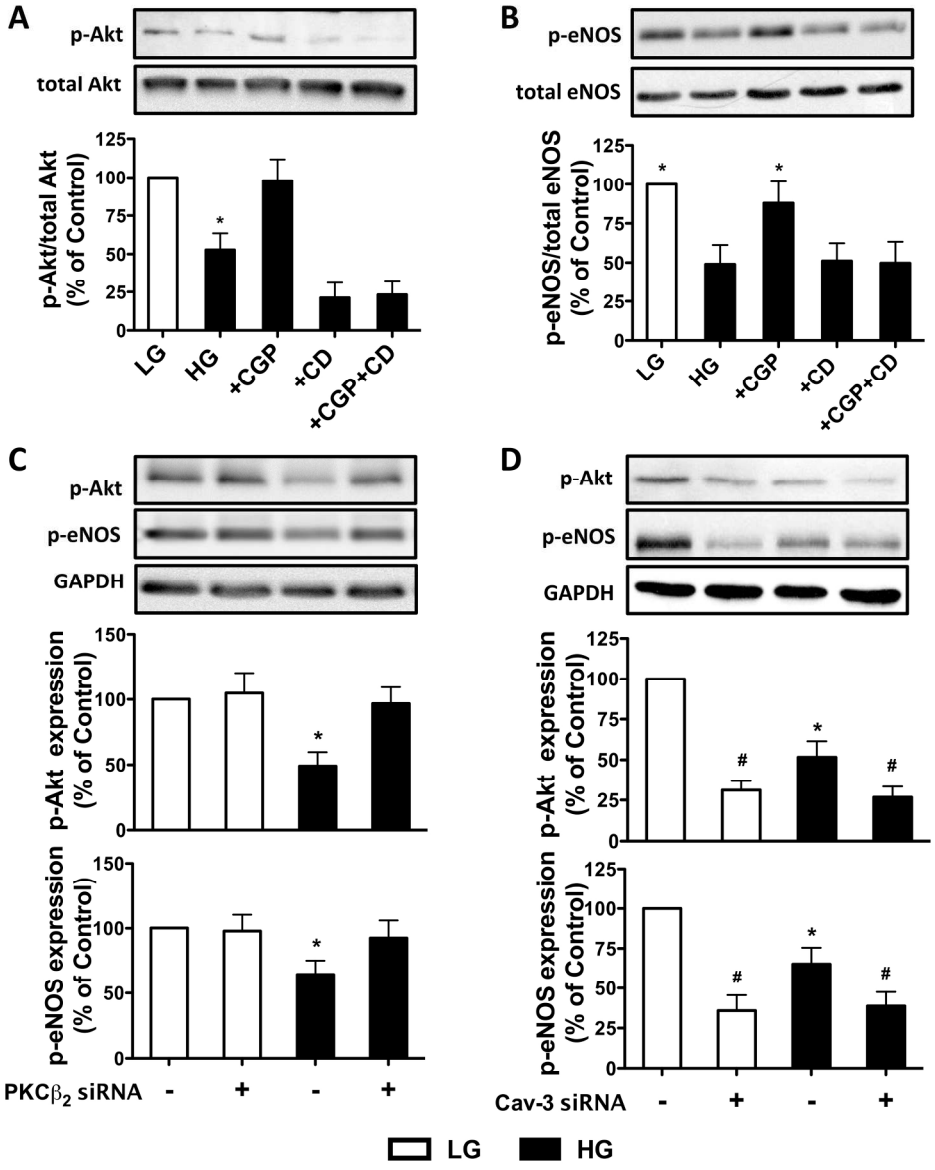

Fig-4
218x264mm (300 x 300 DPI)

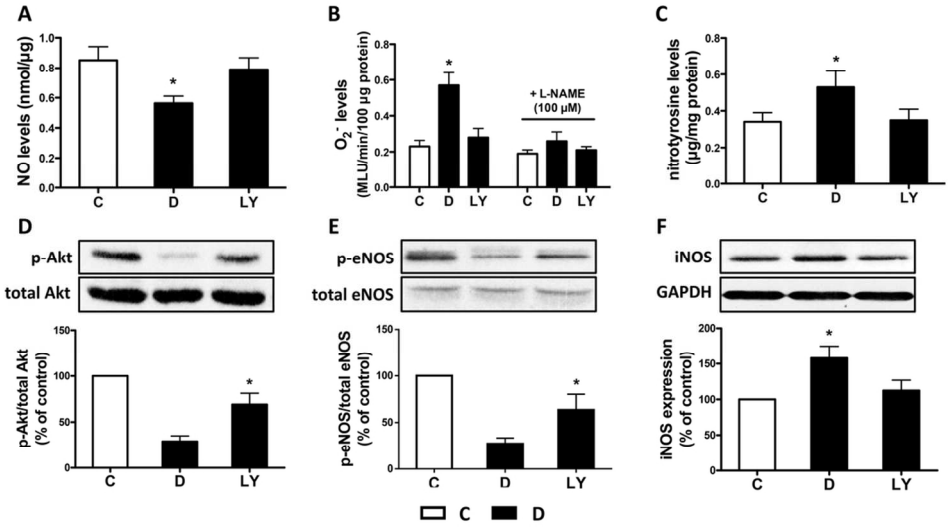

Figure-6
102x57mm (300 x 300 DPI)

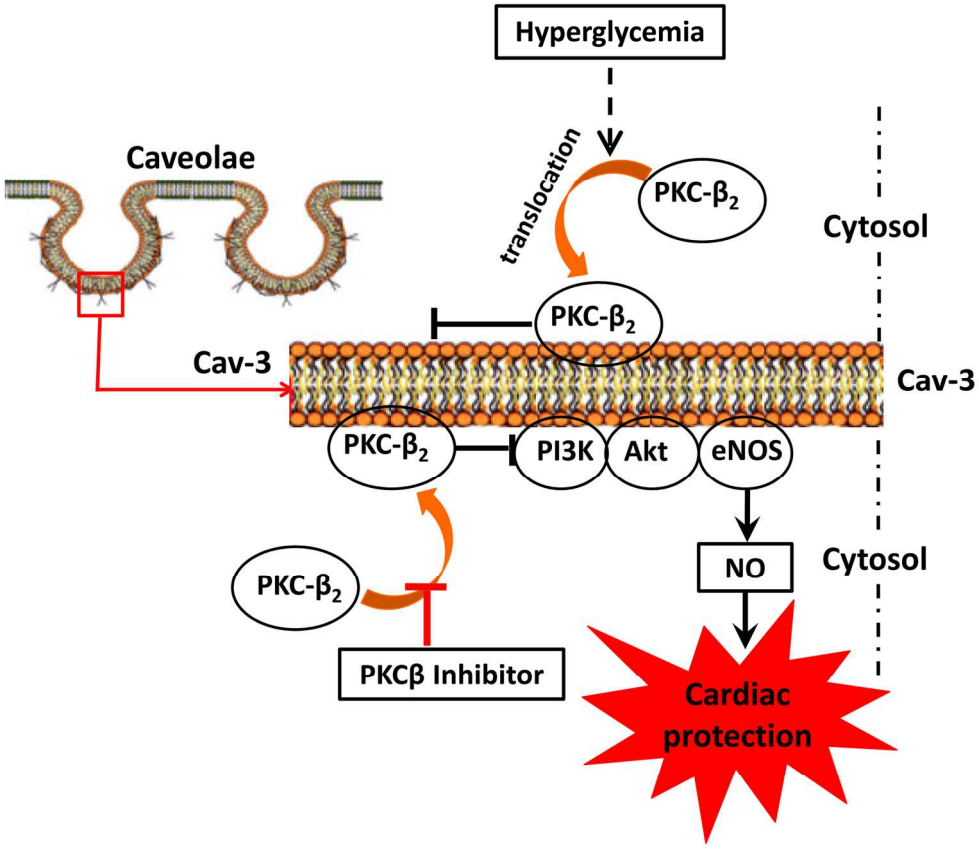

Figure-7
160x142mm (300 x 300 DPI)

Online Appendix

METHODS

Mesurement of cardiomyocytes cross-sectional area

Cardiomyocyte cross-sectional diameters were assessed by H&E (haematoxylin and eosin)-stained paraffin-embedded sections of left ventricles (1–2 μm) longitudinally orientated to the muscle fibers in the subendocardium and subepicardium. Cross-sectional areas were randomly selected in five fields that visualized capillary profiles and nuclei. Images of the left ventricle sections were captured by an Axisoplus image-capturing system (Zeiss) and analysed by Axiovision Rel.4.5 image-analysing software. A minimum of 150 cells per animal were chosen for analysis.

RESULTS

Effects of LY333531 on the left ventricular cardiomyocytes cross-sectional areas

In order to confirm the morphological abnormality of the left ventricles, the cross-sectional areas of cardiomyocyte were used as an indicator of cardiac hypertrophy and were assessed in H&E-stained cardiac sections. As shown in Figure 1, the cross-sectional area in diabetic rats was significantly increased as compared with that in the control group, which was significantly attenuated by LY333531 treatment.

Titles and legends to figures

Figure 1. Effects of LY333531 treatment on the left ventricular cardiomyocytes cross-sectional areas in diabetic rats. The images represent left ventricular cardiomyocytes in control (A), diabetes (B) and diabetes with LY333531 treatment group (C). (D) Quantification of the cross-sectional areas of cardiomyocytes among experimental groups. All results expressed as means ± S.E.M., n=7, $^{*}P<0.05$ vs. all other groups.

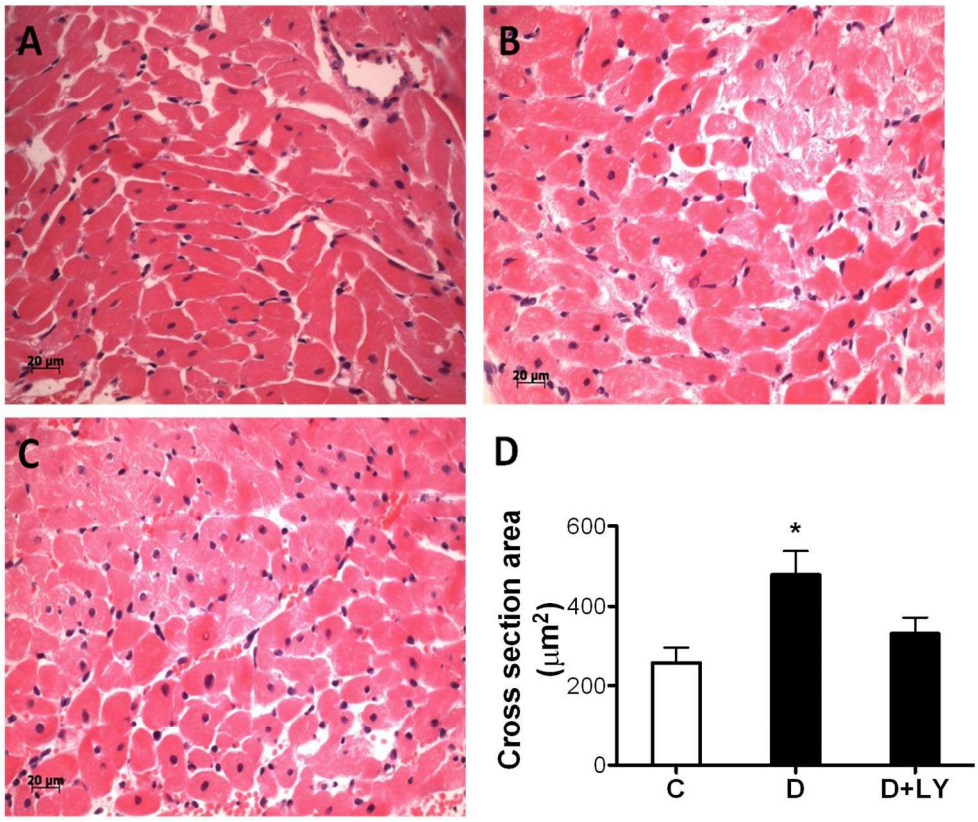

180x150mm (300 x 300 DPI)